Trends in North American net primary productivity derived from satellite observations, 1982–1998

Jeffrey A. Hicke,[1,2] Gregory P. Asner,[1,2] James T. Randerson,[3] Compton Tucker,[4] Sietse Los,[4,5] Richard Birdsey,[6] Jennifer C. Jenkins,[7] and Christopher Field[8]

Received 22 August 2001; revised 4 February 2002; accepted 4 February 2002; published 14 May 2002.

[1] Net primary productivity (NPP) in North America was computed for the years 1982–1998 using the Carnegie-Ames-Stanford approach (CASA) carbon cycle model. CASA was driven by a new, corrected satellite record of the normalized difference vegetation index at 8-km spatial resolution. Regional trends in the 17-year NPP record varied substantially across the continent. Croplands and grasslands of the Central Plains and eastern Canadian forests experienced summer increases in NPP. Peak NPP trends in Alaska and western Canada occurred in late spring or early summer, suggesting an earlier onset of the growing season in these regions. Forests and woodlands of the southeastern United States showed NPP increases in spring and fall, also suggesting an increase in the length of the growing season. An analysis of climate variables showed that summer precipitation increased in the Central Plains, indicating that climate changes probably play some role in increasing NPP in this region, though intensive management of agricultural ecosystems has also increased productivity. Similarly, increased summer precipitation possibly increased NPP in eastern Canada, but another possible explanation is forest recovery after insect damage. NPP in the southeastern United States increased in the absence of climate variation. Much of this region consists of aggressively managed forests, with young stand ages and intensive silviculture resulting in increased NPP. The high latitudes of western Canada and Alaska experienced spring warming that could have increased NPP in late spring or early summer. *INDEX TERMS:* 1615 Global Change: Biogeochemical processes (4805); 1640 Global Change: Remote sensing; 0322 Atmospheric Composition and Structure: Constituent sources and sinks; 1610 Global Change: Atmosphere (0315, 0325); *KEYWORDS:* net primary productivity, North America, trends, carbon cycle, NPP, NDVI

1. Introduction

[2] Net ecosystem productivity (NEP) is the amount of carbon (C) stored by the biosphere, and terrestrial NEP is a major component of the global C cycle. NEP is defined as the difference between net primary productivity (NPP) and heterotrophic respiration (neglecting other terms such as fire and river runoff). Globally, terrestrial NPP and heterotrophic respiration (R_h) are of comparable value, ~60 Pg C yr^{-1} [*Schlesinger*, 1997], whereas the terrestrial C sink is thought to be ~1 Pg C yr^{-1} [*Battle et al.*, 2000; *Bousquet et al.*, 1999]. Since NEP is the small residual of two large terms, it is important to estimate each flux accurately in order to reduce the uncertainty in the value of NEP.

[3] The existence and magnitude of a North American C sink is currently being debated [*Bousquet et al.*, 1999; *Fan et al.*, 1998; *Pacala et al.*, 2001; *Schimel et al.*, 2000]. Various mechanisms causing a North American C sink have been proposed, including CO_2 fertilization, nitrogen (N) deposition, climate change, forest regrowth of abandoned pasture and agricultural lands, and intensive crop and forest management practices [*Houghton et al.*, 1999; *Schimel et al.*, 1995; *Townsend et al.*, 1996]. Studying only the effects of CO_2 fertilization and climate, *Schimel et al.* [2000] argued that CO_2 fertilization is responsible for the majority of their small modeled C sink in the United States, whereas climate changes contribute only a small amount. The larger sink calculated from forest inventories [*Birdsey and Heath*, 1995; *Brown and Schroeder*, 1999] and analysis of historical trends [*Houghton et al.*, 1999] suggest a greater role for land use change and intensive ecosystem management than for CO_2 fertilization and climate change [*Caspersen et al.*, 2000; *Schimel et al.*, 2000]. N deposition could act to stimulate plant growth in ecosystems where N is a limiting resource [*Townsend et al.*, 1996], though its actual impact on NPP over large areas has not been quantified conclusively [*Aber et al.*, 1998; *Nadelhoffer et al.*, 1999].

[4] In this study, we focus on NPP, the pathway by which C enters the biosphere from the atmosphere. All of the mechanisms for the C sink listed above could influence NPP, though this is not necessarily the case. Several types of models have been used to estimate NPP at large spatial scales. Process-based biogeochemical models represent the functioning of plants together with climate and nutrient inputs to compute NPP (e.g., CENTURY, global biome model-biogeochemical cycle (BIOME-BGC), and Terres-

[1]Department of Geological Sciences, University of Colorado, Boulder, Colorado, USA.
[2]Now at Carnegie Institution of Washington, Stanford, California, USA.
[3]Divisions of Geological and Planetary Sciences and Engineering and Applied Science, California Institute of Technology, Pasadena, California, USA.
[4]NASA Goddard Space Flight Center, Laboratory for Atmospheric Physics, Greenbelt, Maryland, USA.
[5]Now at University of Wales, Swansea, UK.
[6]U.S. Department of Agriculture Forest Service, Newtown Square, Pennsylvania, USA.
[7]U.S. Department of Agriculture Forest Service, Burlington, Vermont, USA.
[8]Carnegie Institution of Washington, Stanford, California, USA.

0886-6236/02/2001GB001550

trial Ecosystems Model (TEM) [*Schimel et al.*, 2000]). Production efficiency models calculate NPP from the amount of light absorbed by plants together with a plant light-use efficiency that converts the absorbed energy to carbon uptake [e.g., *Monteith*, 1977; *Ruimy et al.*, 1994]. Production efficiency models often take advantage of available satellite observations of light absorption [*Field et al.*, 1995].

[5] Because of data availability and/or computational expense, continental-scale NPP has been limited to fairly coarse spatial resolution. For example, the model intercomparison study reported by *Cramer et al.* [1999] and a recent study of NPP in the United States [*VEMAP members*, 1995] used a spatial resolution of 0.5°. An exception to this is the Global Production Efficiency Model (GLO-PEM), which has been run at 8-km spatial resolution globally for the period 1982–1989 [*Goetz et al.*, 2000].

[6] Another factor limiting our understanding of NPP is the temporal availability of continental-scale observations. Many studies using production efficiency models, typically driven by satellite observations, have been published using 1 year of data [e.g., *Potter et al.*, 1993; *Ruimy et al.*, 1994]. A few studies considered longer periods, such as *Goetz et al.* [2000] (1980s), *Potter et al.* [1999] (late 1980s), and *Malmström et al.* [1997] (1980s). A limitation to calculating NPP over longer periods has been the challenge of producing a consistent, calibrated normalized difference vegetation index (NDVI) data set needed as input to these models [*Asner*, 2000; *Asner et al.*, 1998]. The short time periods of these studies have limited the certainty with which changes in NPP could be calculated. It is important to understand longer time period variations in NPP to relate those variations to mechanisms that drive the terrestrial C sink.

[7] Here we discuss North American NPP computed over 17 years, 1982–1998, using a new satellite data set and a production efficiency model, the Carnegie-Stanford-Ames approach (CASA) [*Field et al.*, 1995; *Potter et al.*, 1993]. The NDVI has been corrected for satellite artifacts [*Los et al.*, 2000; *Tucker et al.*, 2001] that until now have hindered using such observations over long time periods. Satellite observations have the advantage that actual changes in vegetation are observed and drive changes in NPP. We used spatiotemporal patterns of NPP change together with information on climate to identify regions where NPP may have increased with concomitant changes in precipitation and/or temperature. Using CASA to compute NPP instead of analyzing NDVI alone, as other studies have done for circumpolar regions [*Myneni et al.*, 1997], allowed us to calculate changes in an important carbon cycle flux that can be compared to other biogeochemical and atmospheric inverse modeling results as well as to field measurements of NPP.

2. Model and Data Sets

[8] CASA is a production efficiency model driven by satellite data as well as by temperature, precipitation, solar radiation, and land cover and soil classifications. CASA computes NPP as a function of the absorbed photosynthetically active radiation (APAR), a maximum potential light-use efficiency variable ε^*, and temperature (T_s) and moisture (W_s) scalars that represent climate stresses on vegetation light-use efficiency:

$$\mathrm{NPP} = f\mathrm{APAR}\ \mathrm{PAR}\ \varepsilon^* T_\varepsilon W_\varepsilon, \tag{1}$$

where *f*APAR is the fraction of APAR, solar radiation is converted to PAR by multiplying by 0.5, and *f*APAR × PAR equals APAR. The *f*APAR is determined following *Los et al.* [2000] by using the linear relationships between *f*APAR and NDVI and *f*APAR and the simple ratio (SR):

$$\mathrm{NDVI} = (R_{\mathrm{NIR}} - R_{\mathrm{VIS}})/(R_{\mathrm{NIR}} + R_{\mathrm{VIS}}), \tag{2}$$

$$\mathrm{SR} = R_{\mathrm{NIR}}/R_{\mathrm{VIS}}, \tag{3}$$

where R_{NIR} is the reflectance in the near-infrared channel and R_{VIS} is the reflectance in the visible channel of the advanced very high resolution radiometer (AVHRR). *Los et al.* [2000] found that an average of *f*APAR determined using NDVI and SR compared best with field observations. The processing algorithm [*Los et al.*, 2000; *Tucker et al.*, 2001] corrects NDVI for processes that contaminate the data, such as differences in solar zenith angle, sensor degradation, and missing values. The processed NDVI data, available from 1982 through 1998, are at a spatial resolution of 8 km and have a semimonthly temporal resolution. The two monthly values were averaged to produce the monthly input for CASA. The slopes of the linear relationships between NDVI/SR and *f*APAR were recomputed for each biome following *Los et al.* [2000].

[9] The maximum potential light-use efficiency ε^* (equation (1)) was set by a calibration step where CASA NPP was fit to field observations of NPP; the value of ε^* used in this study was 0.405 [*Potter et al.*, 1993]. Higher values of ε^* have been reported in previous studies using CASA [e.g., *Thompson et al.*, 1996]; higher values will increase NPP and magnify the trends reported here, though the relative increases will not change.

[10] The temperature and moisture scalars (T_s and W_s) were used to reduce the global light-use efficiency (ε^*) in response to climate conditions that act to stress plants beyond what may be resolved in the NDVI [*Field et al.*, 1995]. T_s and W_s were computed at every location at each time step using climate data. Data without missing values throughout the time period of interest in North America were highly desirable to allow interannual variability in the climate variables. National Centers for Environmental Prediction (NCEP) Reanalysis temperatures and solar radiation [*Kistler et al.*, 2001] and Global Precipitation Climatology Project (GPCP) precipitation [*Huffman et al.*, 1997] satisfied this criterion. Both the NCEP and GPCP data sets were at 2.5° resolution and were interpolated to the NDVI 8-km locations. *Hicke et al.* [2002] discuss the sensitivity of the NPP trends to input drivers. They found little large-scale change in the trends when using several different data sets, including satellite-based estimates of solar radiation and data sets at finer scale resolution.

[11] The *Hansen et al.* [2000] 1-km land cover classification, based on 1992–1993 AVHRR data, was aggregated to 8 km to match the NDVI. An additional tundra biome was added to this land cover map using the *DeFries et al.* [1998] classification. The Food and Agriculture Organization/ United Nations Educational, Scientific, and Cultural Organization (FAO/UNESCO) soil map was used to specify soil texture in CASA.

[12] Our North America NPP estimates from CASA were validated against NPP estimated by other studies (J. Hicke et al., North American net primary productivity: Comparisons of modeling and field studies, submitted to *Global Change Biology*, 2001, hereinafter referred to as Hicke et al., submitted manuscript, 2001). The CASA mean NPP compared favorably to values computed from field measurements at Long-Term Ecological Research Network sites [*Knapp and Smith*, 2001], forest inventory data [*U.S. Department of Agriculture Forest Service*, 1992], process-based C cycle models [*Schimel et al.*, 2000], and other production efficiency C cycle models [*Goetz et al.*, 2000].

[13] *Hicke et al.* [2002] showed that NPP trends analyzed in this work compare favorably with those using forest inventory data. They computed NPP with the U.S. Department of Agriculture (USDA) Forest Service Forest Information and Analysis (FIA) data set for four regions in the conterminous United States. Agreement between the CASA and FIA NPP was generally good in the south and east, where inventories were conducted more frequently, and worse in the west, where inventories were less frequent and spatial mismatches occurred between FIA forests and forests identified by the land cover classification. *Lobell et al.* [2002] also showed that

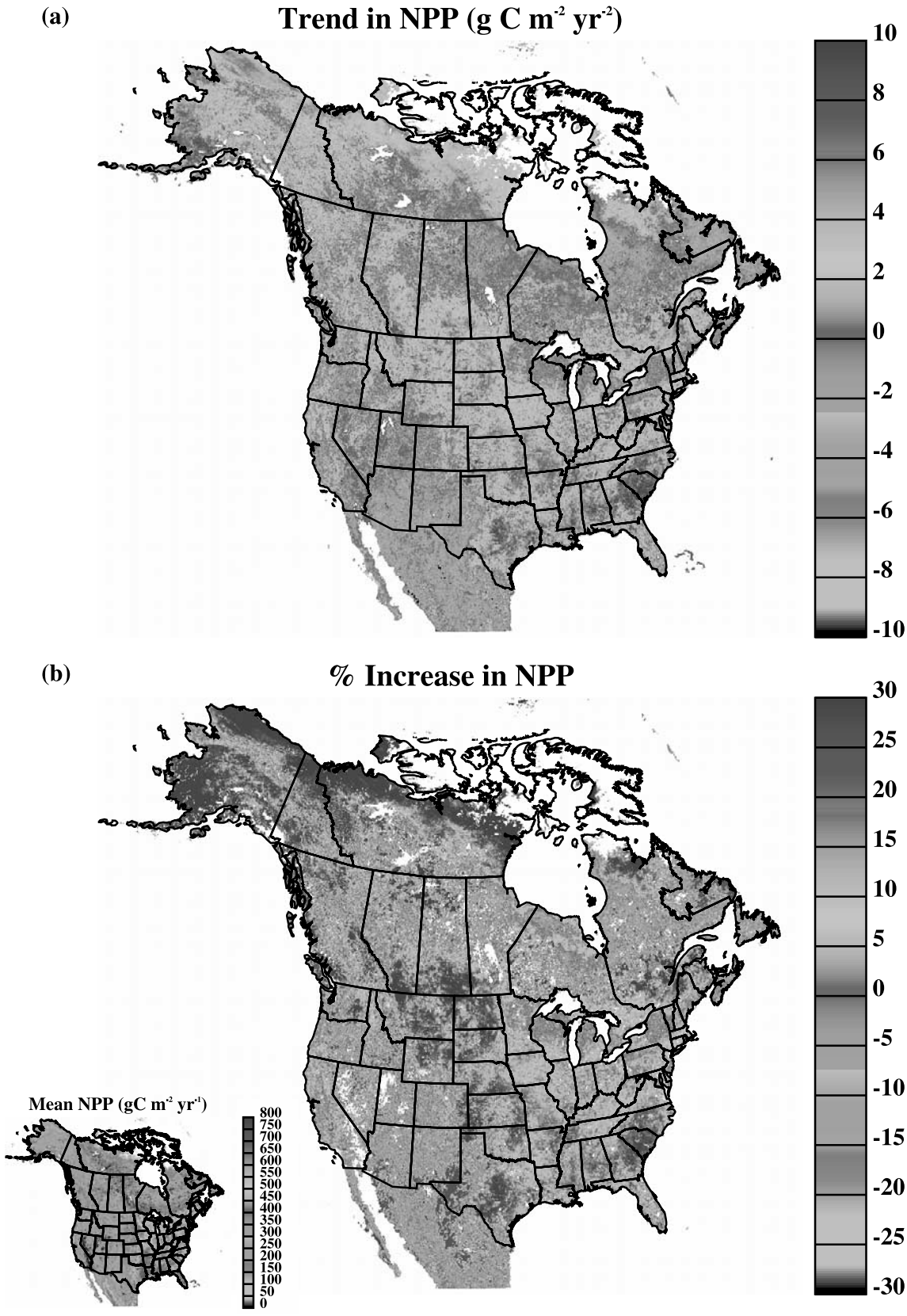

Figure 1. (a) Trends in net primary productivity (NPP, in g C m^{-2} yr^{-2}), 1982–1998. (b) Percentage increase in NPP, computed by multiplying the linear trend at each location by the number of years in the time period (17), then dividing by the 1982 NPP. Inset shows mean annual NPP (in g C m^{-2} yr^{-1}) (taken from Hicke et al., submitted manuscript, 2001). See color version of this figure at back of this issue.

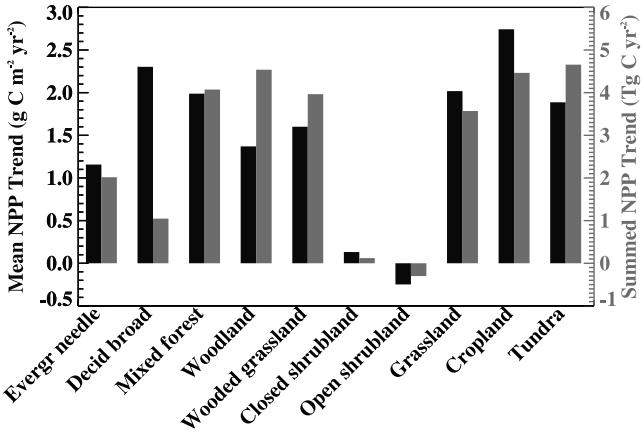

Figure 2. Trends in net primary productivity by biome. Mean per area (in g C m^{-2} yr^{-2}) is shown by black bars with left axis; regional trends (summed across area; in Tg C yr^{-2}) are shown by shaded bars with right axis.

trends in NPP for U.S. croplands matched NPP trends computed using USDA yield data.

3. Annual NPP Trends

[14] We computed a mean total North American annual NPP (i.e., summed across area) of 6.2 Pg C yr^{-1} [*Hicke et al.*, 2002], and the interannual variability was 0.5 Pg C yr^{-1}. A recent atmospheric inverse modeling study discussed North American NEP variability of 1–2 Pg C yr^{-1} [*Bousquet et al.*, 2000], which is 20–40% of our mean NPP. Furthermore, the interannual variability of our NPP estimates is an order of magnitude less than the NEP variability of *Bousquet et al.* [2000], implying that heterotrophic respiration and disturbances such as fire may account for much larger fraction of the NEP variability than NPP. North American NPP increased at a rate of 0.03 Pg C yr^{-2} (significant at the 99% level), corresponding to an increase of 8% in 17 years over the 1982 value [*Hicke et al.*, 2002].

[15] Trends in NPP for the 17 years were computed at each satellite pixel by using linear least squares and are shown in Figure 1a. There is a wide range of trends, and though spatial patterns exist, there is substantial heterogeneity in the results. Regions of large NPP increases occurred in the southeastern United Sates, in the Central Plains of the United States and Canada, in eastern Canada, and along the northwest coast of North America. Negative trends were found in northern Mexico and the southwestern United States and in eastern and central Canada.

[16] Plotting the NPP trends as percentage increases (17-year change divided by 1982 value) (Figure 1b) reveals that changes of 30% or more occurred across the continent. Large percentage increases are evident in Alaska and northern Canada and the Central Plains region, and large relative decreases appeared in central northern Mexico and eastern Canada. Figure 1b suggests that NPP can change dramatically in 17 years. Furthermore, the changes were not uniform across the continent, either absolutely or relatively, implying that the forcing mechanisms must also vary spatially.

[17] NPP trends averaged by biome (in g C m^{-2} yr^{-2}) using the modified land cover classification of *Hansen et al.* [2000] are plotted in Figure 2 (black bars). Values were also summed across area to show the total contribution of each biome to the continental trend (in Tg C yr^{-2}) (shaded bars). Croplands had the largest mean increase in NPP, with deciduous broadleaf forests also having high values. However, the limited areal extent of deciduous broadleaf trees decreased their importance at the continental scale. Shrublands had little or no increase in NPP.

4. Monthly NPP Trends

[18] The map of NPP trends (Figure 1a) shows that although there is large spatial variation, many areas of North America have similar values. Does this imply that areas with similar trends are responding to the same forcing, whether it is climate, CO_2 fertilization, N deposition, or other possible mechanisms? To explore this question, we investigated monthly trends in NPP and climate. All forcing mechanisms related to NPP, including climate, are implicitly accounted for in the NDVI; however, mechanisms other than climate are not directly modeled in CASA. We therefore analyzed monthly trends in model variables by region to determine whether climate plays a role in changing NPP, and if not, we propose other mechanisms of change based on ancillary data.

[19] Monthly trend information allows us to better understand the pattern of NPP change. We calculated the NPP trend for each month of the year by using NPP for all 17 of the Januaries to compute a January trend, all 17 of the Februaries to compute a February trend, and so on. The result was an annual cycle of monthly NPP trends at each location. This annual cycle revealed the time of year when NPP increased or decreased and was useful for assessing whether the annual NPP increases (or decreases) at a given location were due to changes in greenness amplitude or changes in the growing season length (Figure 3).

[20] Figure 4a maps the maximum absolute (positive or negative) monthly NPP trend at each location, and Figure 4b displays the month in which this maximum occurs. The largest monthly trends occurred in the central United States, Texas, and Alaska. Large positive values are evident throughout much of North America, particularly on the coasts, in the southeastern United States, and in northern Alaska and Canada. Negative monthly trends were strongest in northern Mexico, eastern Canada, and across central Canada.

[21] The high latitudes tended to have the largest NPP changes during May and June. For the regions where NPP was increasing,

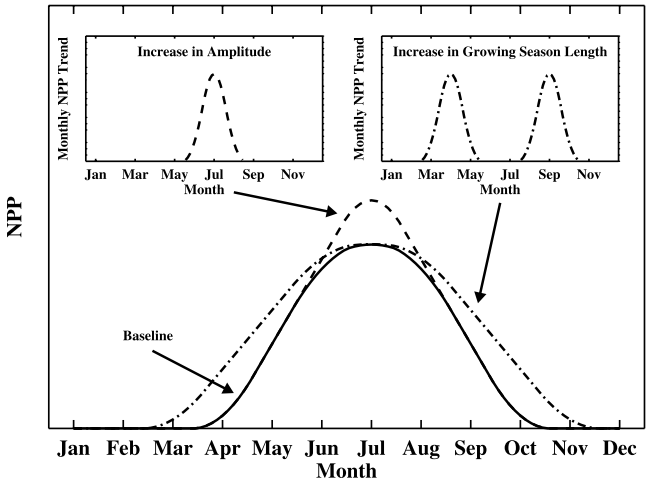

Figure 3. Schematic showing monthly trends in net primary productivity (NPP) in response to an increase in the amplitude of the NPP annual cycle (dashed curve) and an increase in the length of the growing season (dash-dotted curve) from a baseline NPP annual cycle (solid curve).

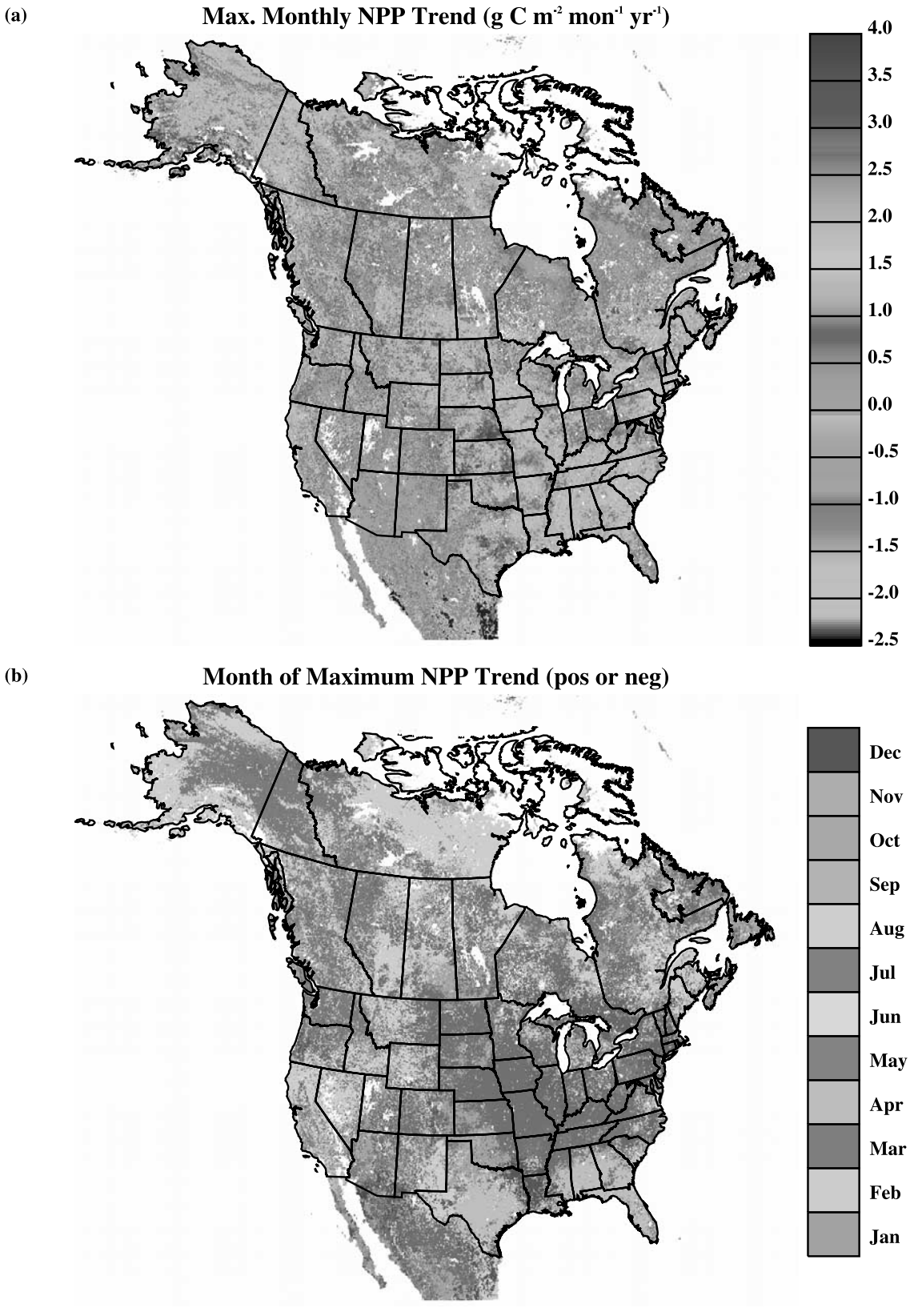

Figure 4. (a) Maximum monthly trend in net primary productivity (NPP, in g C m^{-2} $month^{-1}$ yr^{-1}). Monthly trends were computed for each month (January, February, etc.), generating an annual cycle of monthly trends at each point. This plot shows the maximum absolute value (positive or negative) of the monthly trends at each point. (b) Month when maximum absolute value (positive or negative) of monthly NPP trend occurred. See color version of this figure at back of this issue.

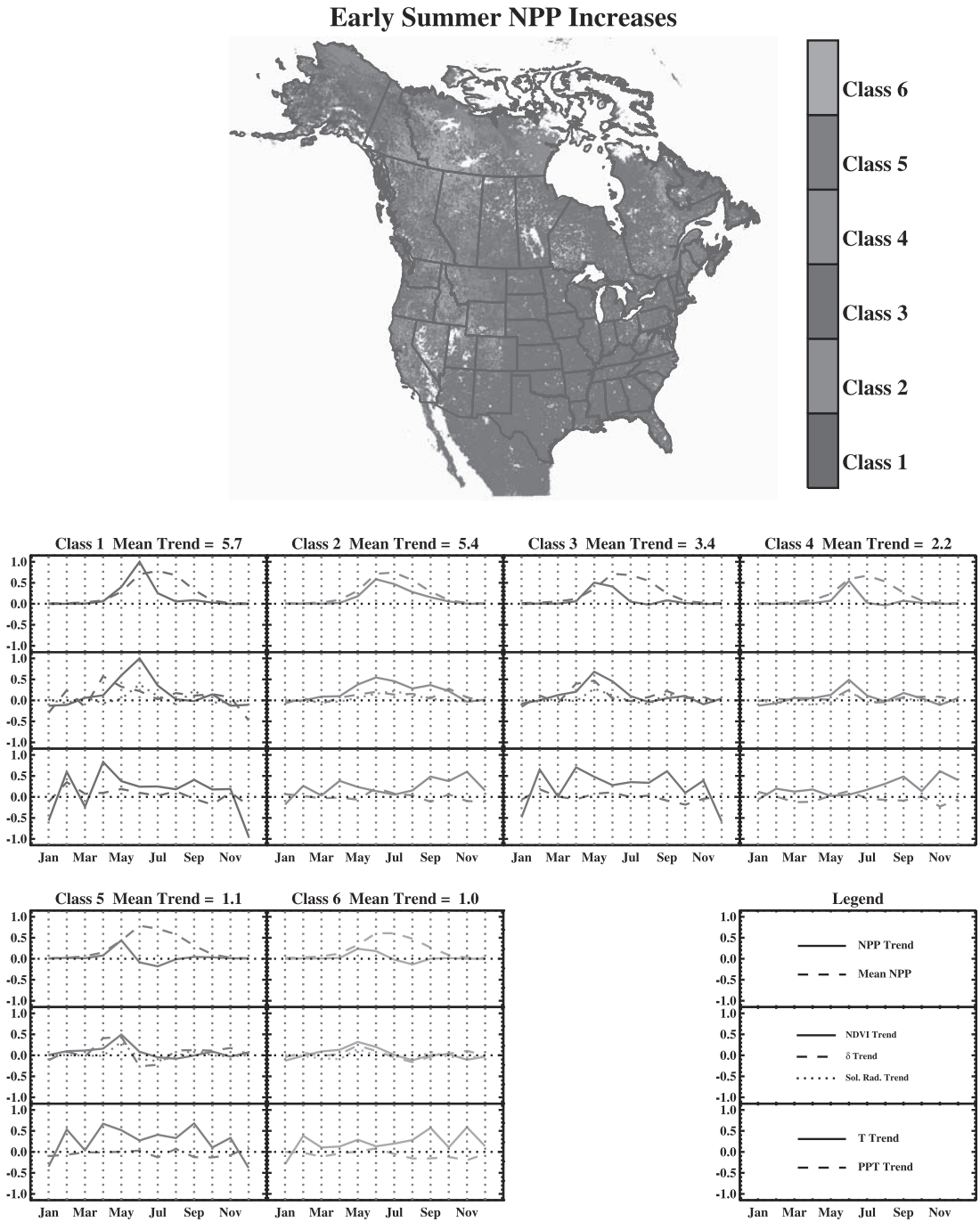

Figure 5. Results of a classification based on monthly net primary productivity (NPP) and climate trends; see text for details of the method. (Top) Map of locations of Classes 1–6, which have early summer NPP increases. (Bottom) Annual cycle of variables associated with each class, averaged across all points associated with that class. Top panel in each plot shows mean monthly trend in NPP (solid curve) and mean monthly NPP (dashed curve). Middle panel in each plot shows trends in NDVI (solid curve), climate down-regulator δ (dashed curve), and solar radiation (dotted curve). Bottom panel in each plot shows mean monthly trends in temperature (solid curve) and precipitation (dotted curve). All variables are normalized by largest value across classes. See color version of this figure at back of this issue.

this corresponds to earlier onset of the growing season (Figure 3). The large monthly NPP trends seen in the central United States and Canada occurred during the summer months (Figure 4b), indicating an increase in the amplitude of NPP. The south central, southeastern, and eastern United States had maximum monthly NPP trends in April and October; the growing season appears to be lengthening here as well as at high latitudes.

[22] To further investigate the seasonal dynamics of NPP, we classified monthly NPP and climate trends to group locations having similar behavior. This isolated regions that had length-

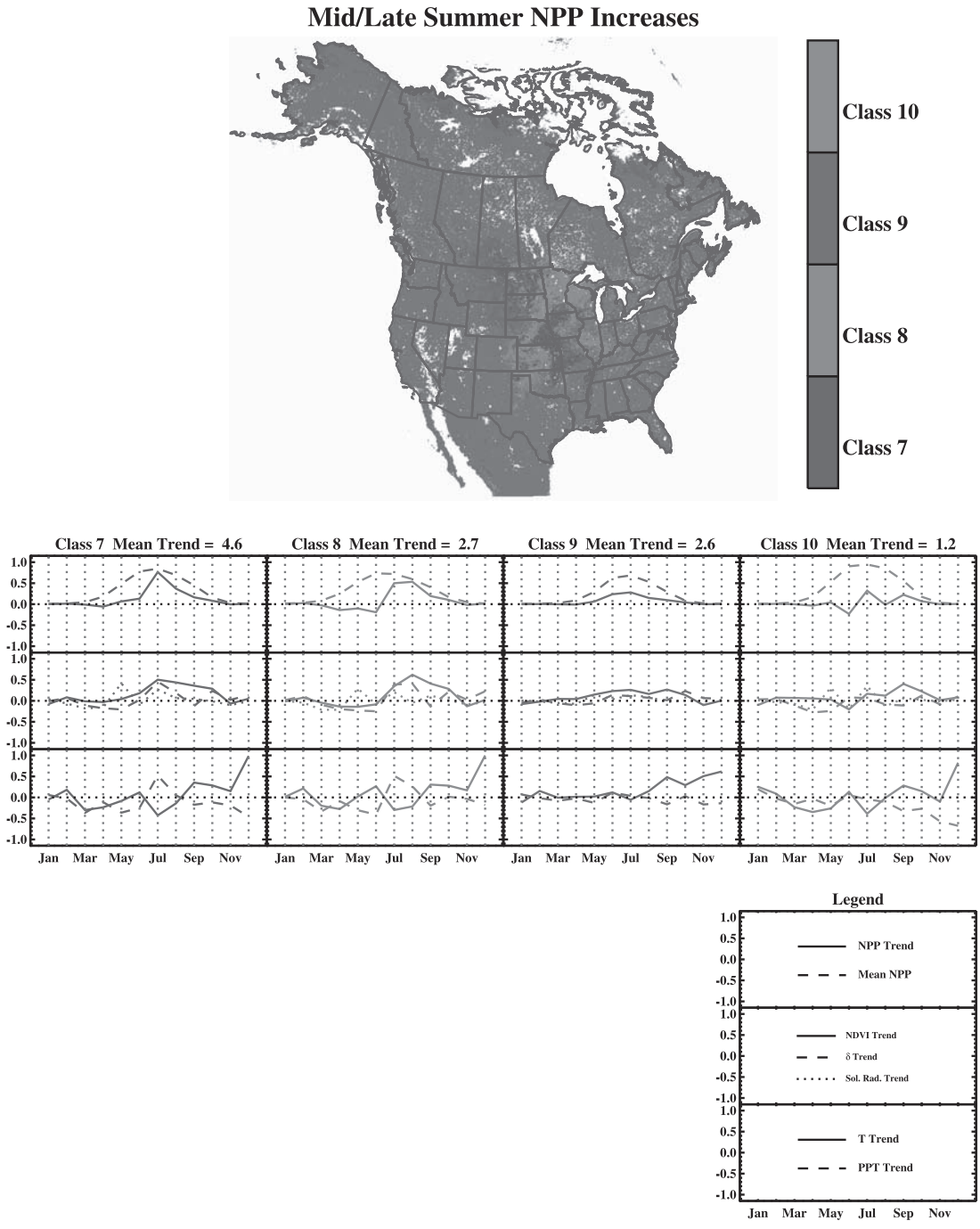

Figure 6. Same as Figure 5, but for classes with mid- and/or late summer increases in NPP. See color version of this figure at back of this issue.

ening growing seasons, for example, or had increased NPP in summer. The light-use efficiency down-regulator, δ, is the modeled stressor on plant growth resulting from climate:

$$\delta = T_\varepsilon W_\varepsilon, \tag{4}$$

where T_s and W_s are from equation (1). Increases in d result in increases in NPP. We used d in the classification as an index of climate-driven impacts on vegetation productivity. The monthly NPP and δ trends were first normalized to allow these variables to be used together in the classification.

[23] The k-means algorithm [*Hartigan*, 1975] classifies locations to minimize errors in the Euclidean distance from the class mean. The algorithm requires the number of classes as input. Because of the large number of satellite pixels, the NPP response across North America varies considerably, and thus we specified 20 classes. Specifying fewer classes hid some details in the analysis; additional classes made interpretation difficult. Although the classification assigns each pixel to a class and although we present class mean information, we emphasize that a pixel may not behave in a manner close to the class mean. Thus we focus our results on the large-scale patterns that occurred. We grouped the

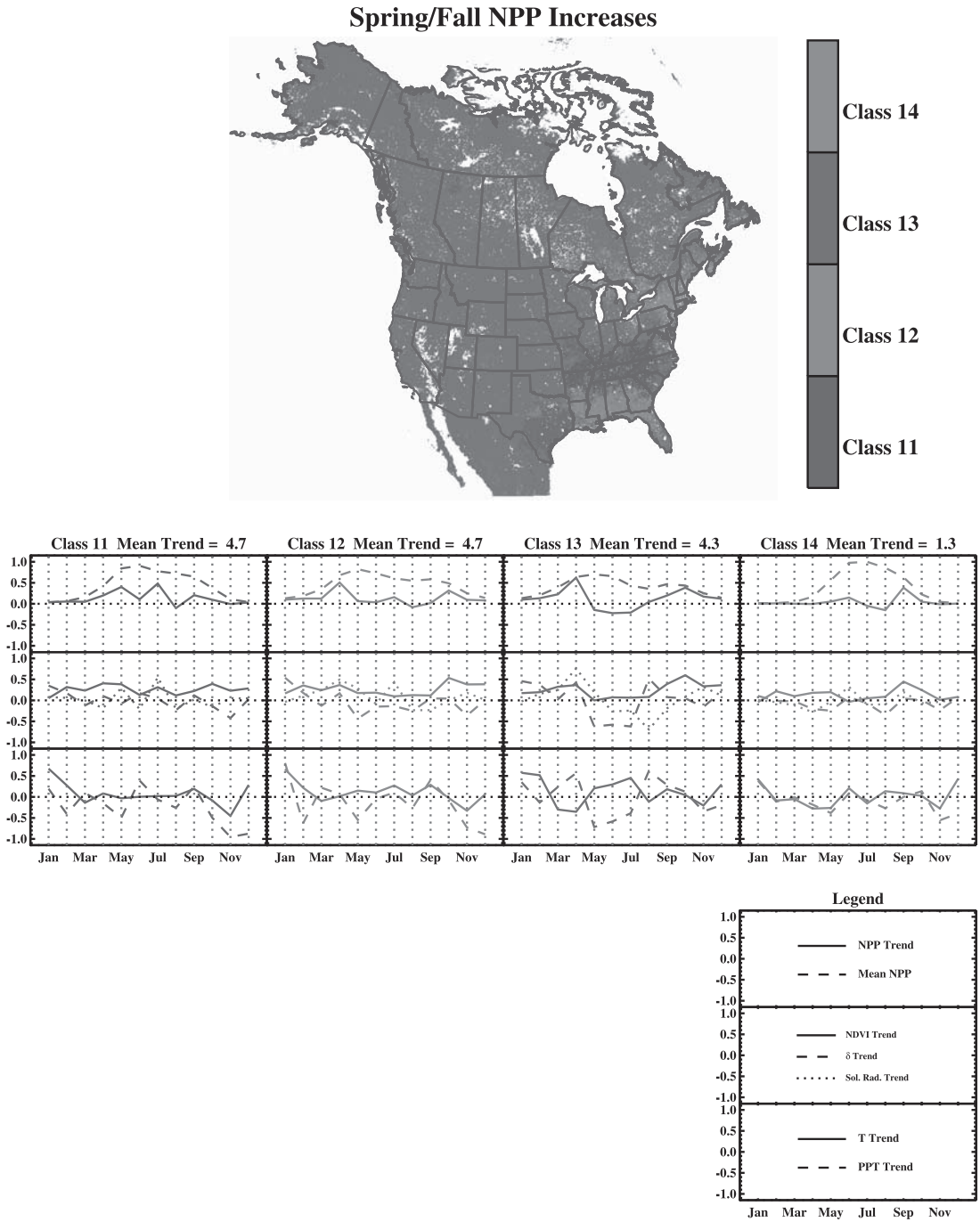

Figure 7. Same as Figure 5, but for classes with spring and fall increases in NPP. See color version of this figure at back of this issue.

resulting classes into four general categories: early summer increases in NPP, middle and late summer increases, spring and fall increases, and little change or decrease in NPP. This categorization is necessarily approximate; several classes could belong to two categories. However, we present the categories as an aid in interpreting the large-scale behavior.

[24] For each category, we plot the locations associated with the different classes (Figures 5, 6, 7, and 8). In addition, we plot the annual cycles of NPP, light-use efficiency down-regulator δ, temperature, precipitation, solar radiation, and NDVI, averaged across locations associated with each class. The mean monthly NPP trends and mean monthly NPP are shown in the top panel of each plot. In the middle panel of each plot we show mean monthly trends in δ, NDVI, and solar radiation; these influence NPP through equation (1). The bottom panel of each plot shows the mean monthly trends in temperature and precipitation. Note that temperature and precipitation affect NDVI as well as δ. Plotting these variables allowed us to observe which climate factor (temperature, precipitation, or solar radiation) drove changes in NPP and δ, as well as allowing us to see when NDVI was changing independ-

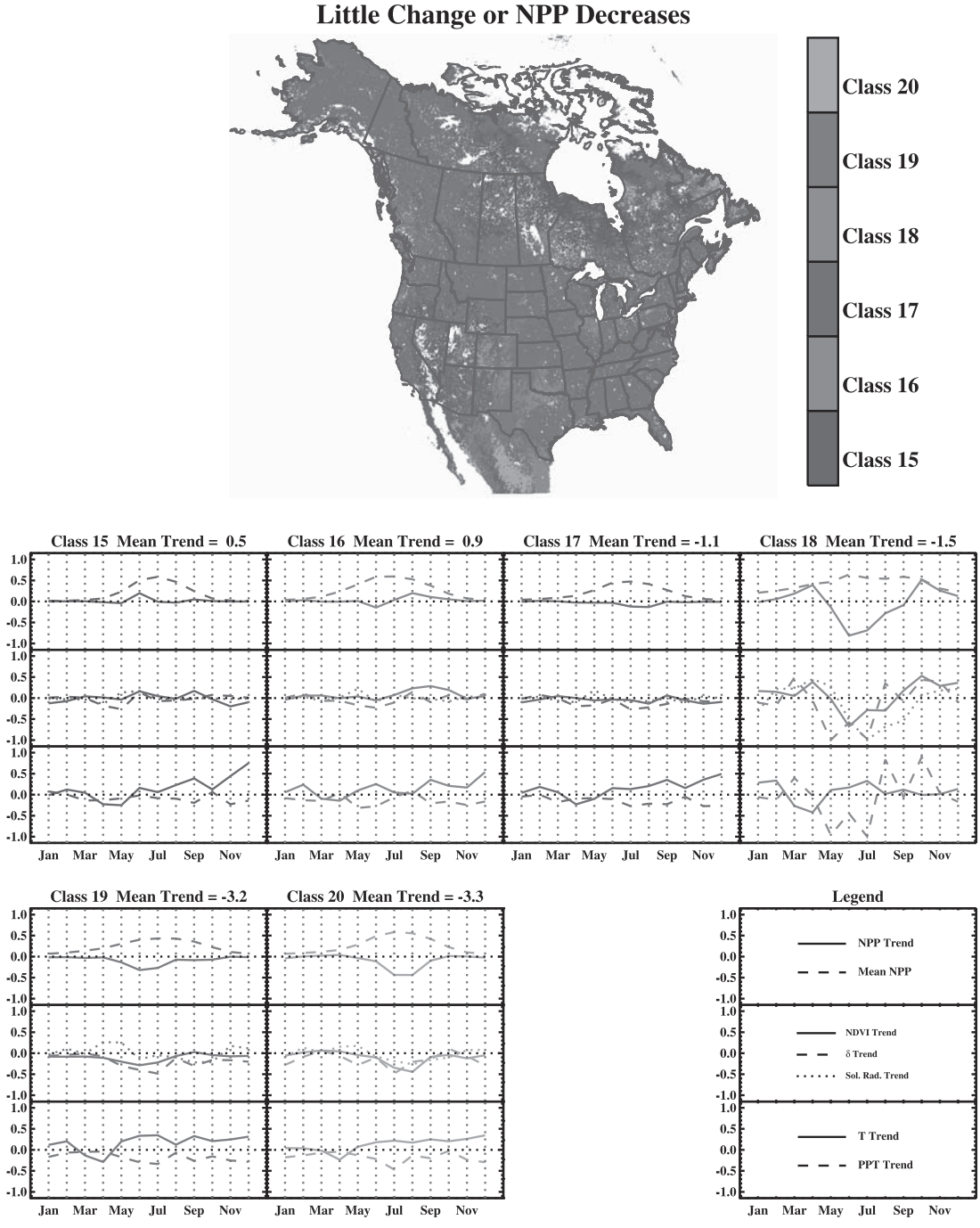

Figure 8. Same as Figure 5, but for classes with little change or decreases in NPP. See color version of this figure at back of this issue.

ent of climate changes. All variables were plotted after normalizing to the largest mean values of all classes in order to highlight the relative magnitudes between classes. The trend in annual NPP (Figure 1a) averaged across the locations of each class is printed at the top of each time series plot. The classification based on NPP and δ monthly trends resulted in pixels that in general, were grouped together spatially, resulting in similar temporal pattern of the climate variables within a class. For a small number of classes, however, wide geographic separation of the class may mean that the climate behavior is somewhat different between these regions.

[25] Locations with NPP increases in early summer (Classes 1–6) are shown in Figure 5. Much of western and northern North America was associated with this category; other regions include parts of eastern North America and northern Canada. The largest annual NPP trends of this category were located in southwestern Alaska (Class 1). Class 1 δ trends were strongly positive in spring and early summer and were associated with increases in temperature. Similar patterns in NPP and climate trends were evident in the other classes (Classes 2–6), though with reduced magnitude. The spatial and temporal patterns of Classes 1–6 were consistent with a lengthening growing season due to early spring warming

postulated by past studies [*Keeling et al.*, 1996; *Myneni et al.*, 1997; *Randerson et al.*, 1999]. Tundra and woodlands were the most numerous biomes in this category (Figure 9). Class 2 also encompasses regions in Montana and eastern Canada. These two regions had NPP increases throughout summer, and so Class 2 could also be placed in the category of middle and late summer increases (category 2).

[26] The second category (Figure 6) contains locations that had NPP increases in middle and late summer and generally occurred in the Central Plains. Climate appears to play a role in the summer increases for Classes 7 and 8, since these had increases in precipitation. However, since croplands and grasslands made up most of these locations (Figure 9), another contributor probably was increasing yields resulting from agricultural practices [*Lobell et al.*, 2002] (see also U.S. Department of Agriculture, Published Estimates Database, National Agricultural Statistics Service, available at http://www.nass.usda.gov:81/ipedb/ 2001, hereinafter referred to as USDA Published Estimates Database). Class 9 also contains locations at the highest latitudes, where NPP increased in June.

[27] The third category groups classes that had NPP increases in spring and/or fall (Figure 7). Locations in the Gulf Coast region of the southern and southeastern United States formed three of the classes. The western region, Class 13, appears to be driven by climate in the form of precipitation increases in the spring and fall and decreases during summer. In contrast, the southeastern United States (Classes 11 and 12) had NPP increases in spring and fall that appear to be somewhat independent of climate driving factors. *Hicke et al.* [2002] showed that this region's large increases computed by CASA were matched by increases calculated using forest inventory data.

[28] The last category (Figure 8) shows where NPP was unchanging or decreasing. Two main regions are evident, northern Canada and the southwestern United States and northern Mexico. NPP decreases were accompanied by shifts to a less favorable climate in the 1980s and 1990s.

5. Discussion

[29] With the currently available data, it is not possible to say with certainty if climate has driven NPP increases across North America, but it appears that climate is a factor that must be considered when explaining these increases. Many of the locations exhibiting increasing NPP had plausible explanations based on climate shifts, such as that the pronounced spring increase in NPP at high latitudes followed noticeable spring warming (Figure 10). Decreases in NPP typically occurred in conjunction with changes to a less favorable climate for plant growth. In the American Southwest, reduced precipitation impacted NPP, whereas at high latitudes, decreased temperatures also played a role.

[30] In some regions, NPP increases could be due to several mechanisms. For example, the large positive NPP trend in the Central Plains could be a result of increased precipitation during summer. However, another mechanism could be that this region has experienced increased productivity as a result of intensive crop management [*Lobell et al.*, 2002] (see also USDA Published Estimates Database).

[31] NPP increased in several regions where climate showed little trend, implying that other mechanisms were at work. The southeastern United States, for example (Classes 11 and 12), had dramatic NPP trends in spring and fall, but had only small trends in precipitation and temperature. The young stand age of pine plantations in this region reported by the FIA [*Sheffield and Dickson*, 1998] and the immature hardwood forests found by *Brown et al.* [1997] have likely contributed to this NPP increase. Pine stocking of forests makes up >50% of timberland in many of the Southern states [*Sheffield and Dickson*, 1998], and much of the southern pine stands are below maximum aboveground productivity [*Allen et al.*, 1990]. Intensive management of the southern pine forests, including increased use of genetically improved planting stock, is increasing productivity [*Allen et al.*, 1990].

[32] Recovery of forests from abandoned cropland or disturbance could act to increase NPP. Several studies showed that NPP increases in stands for decades after the disturbance [*Gower et al.*, 1996; *Ryan et al.*, 1997], and *Caspersen et al.* [2000] used forest inventory data to show that land use change is the primary cause behind the C sink in U.S. forests. Increases in forest cover have been documented, using the FIA data, in the southeastern United States, a region of strong NPP increases apparent from satellite observations (Figure 1a) [*Smith et al.*, 2002].

[33] Regrowing forests may be important contributors to increased NPP in eastern Canada, where NPP increased in summer and where climate trends may not be important (e.g., Class 2 and, to a lesser extent, Classes 4 and 9). *Williams and Liebhold* [2000] showed that the region with the most number of years of spruce budworm outbreaks from 1945 to 1988 occurs around the mouth of the St. Lawrence River in eastern Canada. NPP in this region calculated with CASA increased throughout the summer.

[34] NPP trends were very high in the southwestern part of Class 2 in Montana and Alberta. There was a suggestion of an increase in precipitation in this region, but it was not as strong as seen in other regions with similar patterns of NPP increases, such as in the central United States. A large percentage of this region is grassland and cropland; changes in agricultural practices such as irrigation or fertilization could be driving these NPP increases [*Dyson*, 1999].

[35] Mechanisms other than climate or intensively managed ecosystems also could play a role in driving observed trends in NDVI and subsequent increases in modeled NPP. CO_2 fertilization has been suggested as an important cause of increases in plant productivity [*Schimel et al.*, 1995], though recent evidence suggests that postdisturbance forest regrowth is the dominant factor [*Caspersen et al.*, 2000; *Schimel et al.*, 2000]. Our map of NPP trends suggests that if CO_2 is having an impact, its effect is not constant across the continent, even on a percentage increase basis, consistent with both theoretical and experimental studies [*Bolker et al.*, 1995; *Friedlingstein et al.*, 1995; *Oechel et al.*, 1994].

[36] Nitrogen (N) deposition has also been suggested as a way to increase NPP through fertilization of N-limited ecosystems. Our pattern of NPP increase does not match a map of N deposition [*Townsend et al.*, 1996], which occurs primarily in the eastern and northeastern United States. Little or no change in NPP is seen these regions. The lack of a signature of N deposition on NPP is corroborated by field studies of N deposition reporting that very little added N is found in vegetation [*Aber et al.*, 1998; *Nadelhoffer et al.*, 1999]. Lack of an N deposition signal may also be the result of cooccurring stressors such as tropospheric ozone and acid deposition [*Mickler et al.*, 2000].

[37] A final possible explanation, though highly speculative, is shifts in species compositions. If a species that is substantially more productive increases in number, such as red maple on the east coast of the United States, the resulting positive trends in productivity might be seen at the satellite pixel scale. NPP computed using CASA is primarily driven by NDVI, and is only slightly sensitive to variations in climate inputs. *Hicke et al.* [2002] demonstrated that using different climate inputs resulted in similar NPP behavior. Whereas temperature and precipitation effects do not vary much between different climate data sets (though the effects of finer spatial resolution can be seen), greater NPP variation resulted from different solar radiation data sets. From Figures 5, 6, 7, and 8 it can be seen, however, that the NCEP solar radiation trends did not influence NPP trends substantially. Thus we believe that the broad, large-scale patterns depicted in Figure 10 are robust features that are not sensitive to

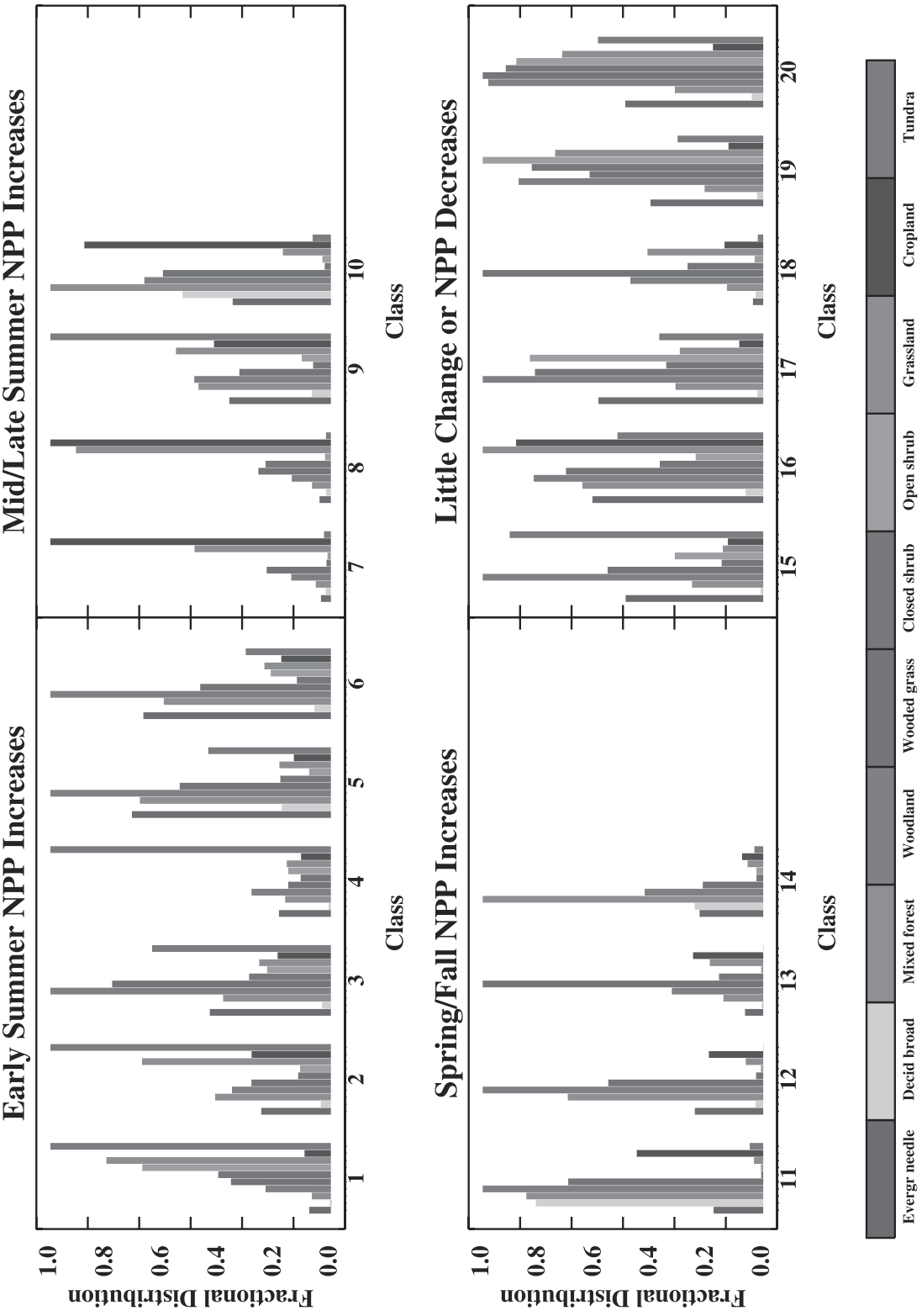

Figure 9. Fractional frequency distribution of biomes within each class. See color version of this figure at back of this issue.

the
cli-

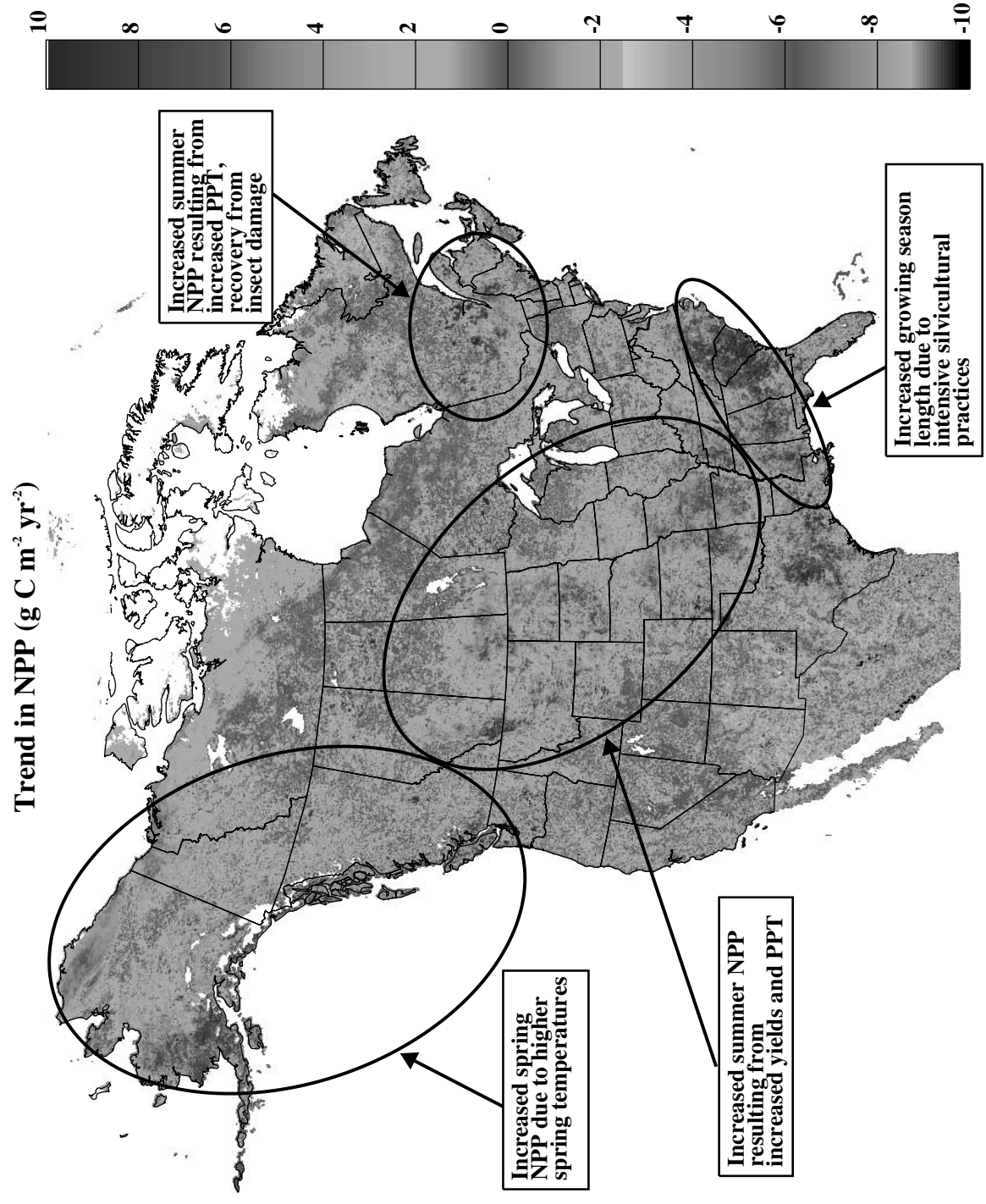

Figure 10. Same as Figure 1a, with additional summaries of regions where NPP has increased. Seasonal timing of NPP increase is indicated as well as possible explanations (CO_2 fertilization is not considered). See color version of this figure at back of this issue.

mate drivers used. Fine-scale patterns may change, however, as the community develops reliable, fine spatial scale data sets such as the Vegetation/Ecosystem Modeling and Analysis Project (VEMAP) input drivers of temperature, precipitation, and solar radiation (T. G. F. Kittel et al., VEMAP Phase 2 Historical and Future Scenario Climate Database, available from the VEMAP Data Group, National Center for Atmospheric Research, at http://www.cgd.ucar.edu/).

6. Conclusions

[38] A new, long-term satellite NDVI record was used to compute NPP over North America at high spatial resolution. Together with the CASA carbon cycle model, we investigated where and when NPP increased, identified regions showing similar NPP behavior, and assessed the contribution of shifts in climate that could account for calculated NPP patterns.

[39] Substantial variations occurred in the NPP changes. The regions containing the largest increases in NPP were the southeastern United States, Central Plains, and east and west coasts of Canada as well as Alaska. Decreases in NPP occurred in northern Canada and the American Southwest.

[40] Monthly trends in NPP revealed that large areas in northwestern Canada and Alaska had NPP increases in late spring and early summer, providing evidence of a lengthening growing season as predicted by past studies [*Keeling et al.*, 1996; *Myneni et al.*, 1997; *Randerson et al.*, 1999]. Regions in the southeast United States also experienced a lengthened growing season, where NPP increased not only in spring but also in fall. In contrast, the large NPP increases in the Central Plains occurred during the middle of summer, increasing the amplitude of the NPP annual cycle.

[41] These results were reinforced by the classification of locations based on monthly NPP trends. Furthermore, the classification suggested that changes in climate appear to play a part in the NPP changes in some regions but not others and that different components of climate (temperature versus precipitation) drive NPP changes in different regions. The NPP increase at high latitudes in western Canada and Alaska was likely to be driven by the spring increases in temperature. Other regions also had NPP changes that were probably a result of changes in precipitation, as in Texas.

[42] In contrast, the southeastern United States showed evidence of NPP increases in the absence of strong climate trends. Since this region is dominated by intensively managed forests, it is likely that NPP increases were caused by silvicultural practices such as changes in species composition as well as by shifts toward younger stand ages resulting from harvesting [*Sheffield and Dickson*, 1998].

[43] The effect of CO_2 fertilization cannot be quantified from our study since any resulting changes were implicit in the satellite observations and were not explicitly modeled. Lack of a broad CO_2-fertilization response in NDVI and thus in our computed NPP is not surprising. Field studies show strong constraints over NPP responses to CO_2 that vary by vegetation type, climate regime, nutrient availability, and other factors [*DeLucia et al.*, 1999; *Oren et al.*, 2001; *Smith et al.*, 2000]. Our calculated NPP did not show evidence of N deposition, which is highest in the northeastern United States. Regrowth of forests after abandonment or disturbance may play a significant role in increasing NPP estimated in this study. However, the quantification of impacts attributable to this process requires detailed information about disturbance and requires more research in this area.

[44] In summary, we found a wide range of NPP responses, both spatially and seasonally. It appears that climate played a role in many regions, but not in others. Therefore, it is very unlikely that a proposed North American C sink can be attributed to one specific factor.

[45] **Acknowledgments.** This work was funded by NASA OES grants NAG5-9356 and NAG5-9462 and by NASA NIP grant NAG5-8709. VEMAP and the Ecosystem Dynamics and the Atmosphere Section, National Center for Atmospheric Research, supplied VEMAP climate data.

References

Aber, J., W. McDowell, K. Nadelhoffer, A. Magill, G. Berntson, M. Kamakea, S. McNulty, W. Currie, L. Rustad, and I. Fernandez, Nitrogen saturation in temperate forest ecosystems: Hypotheses revisited, *Bioscience*, *48*(11), 921–934, 1998.

Allen, H. L., P. M. Dougherty, and R. G. Campbell, Manipulation of water and nutrients: Practice and opportunity in southern United States pine forests, *For. Ecol. Manage.*, *3*(1–4), 437–453, 1990.

Asner, G. P., Contributions of multi-view angle remote sensing to land-surface and biogeochemical research, *Remote Sens. Rev.*, *18*, 137–162, 2000.

Asner, G. P., B. H. Braswell, D. S. Schimel, and C. A. Wessman, Ecological research needs from multiangle remote sensing data, *Remote Sens. Environ.*, *63*, 155–165, 1998.

Battle, M., M. L. Bender, P. P. Tans, J. W. C. White, J. T. Ellis, T. Conway, and R. J. Francey, Global carbon sinks and their variability inferred from atmospheric O_2 and ^{13}C, *Science*, *287*, 2467–2470, 2000.

Birdsey, R. A., and L. S. Heath, Carbon changes in U.S. forests, in *Productivity of America's Forests and Climate Change*, edited by L. A. Joyce, pp. 56–70, U.S. Dep. Agric. For. Serv., Rocky Mountain For. Range Exp. Stn., Fort Collins, Colo., 1995.

Bolker, B. M., S. W. Pacala, F. A. Bazzaz, C. D. Canham, and S. A. Levin, Species diversity and ecosystem response to carbon dioxide fertilization: Conclusions from a temperate forest model, *Global Change Biol.*, *1*, 373–381, 1995.

Bousquet, P., P. Peylin, P. Ciais, M. Ramonet, and P. Monfray, Inverse modeling of annual atmospheric CO2 sources and sinks, 2, Sensitivity study, *J. Geophys. Res.*, *104*(D4), 26,179–26,193, 1999.

Bousquet, P., P. Peylin, P. Ciais, C. Le Quere, P. Friedlingstein, and P. Tans, Regional changes in carbon dioxide fluxes of land and oceans since 1980, *Science*, *290*, 1342–1346, 2000.

Brown, S. L., and P. E. Schroeder, Spatial patterns of aboveground production and mortality of woody biomass for eastern US forests, *Ecol. Appl.*, *9*(3), 968–980, 1999.

Brown, S., P. Schroeder, and R. Birdsey, Aboveground biomass distribution of US eastern hardwood forests and the use of large trees as an indicator of forest development, *For. Ecol. Manage.*, *96*, 37–47, 1997.

Caspersen, J. P., S. W. Pacala, J. C. Jenkins, G. C. Hurtt, P. R. Moorcraft, and R. A. Birdsey, Contributions of land-use history to carbon accumulation in U. S. forests., *Science*, *290*, 1148–1151, 2000.

Cramer, W., D. W. Kicklighter, A. Bondeau, B. Moore III, G. Churkina, B. Nemry, A. Ruimy, A. L. Schloss, J. Kaduk, and the participants of the Potsdam NPP Intercomparison, Comparing global models of terrestrial net primary productivity (NPP): Overview and key results, *Global Change Biol.*, *5*(Suppl. 1), 1–15, 1999.

DeFries, R. S., M. Hansen, J. R. G. Townshend, and R. Sohlberg, Global land cover classifications at 8 km spatial resolution: The use of training data derived from Landsat imagery in decision tree classifiers, *Int. J. Remote Sens.*, *19*, 3141–3168, 1998.

DeLucia, E. H., et al., Net primary production of a forest ecosystem with experimental CO^2 enrichment, *Science*, *284*, 1177–1179, 1999.

Dyson, T., World food trends and prospects to 2025, *Proc. Natl. Acad. Sci. U. S. A.*, *96*(11), 5929–5936, 1999.

Fan, S., M. Gloor, J. Mahlman, S. Pacala, J. Sarmiento, T. Takahashi, and P. Tans, A large terrestrial carbon sink in North America implied by atmospheric and oceanic carbon dioxide data and models, *Science*, *282*, 442–446, 1998.

Field, C. B., J. T. Randerson, and C. M. Malmström, Global net primary production: Combining ecology and remote sensing, *Remote Sens. Environ.*, *51*, 74–88, 1995.

Friedlingstein, P., I. Fung, E. A. Holland, J. John, G. Brasseur, D. Erikson, and D. Schimel, On the contribution of the biospheric CO_2 fertilization to the missing sink, *Global Biogeochem. Cycles*, *9*, 541–556, 1995.

Goetz, S. J., S. D. Prince, J. Small, and A. C. R. Gleason, Interannual variability of global terrestrial primary production: Results of a model driven with satellite observations, *J. Geophys. Res.*, *105*(D15), 20,077–20,091, 2000.

Gower, S. T., R. E. McMurtrie, and D. Murty, Aboveground net primary production decline with stand age: Potential causes, *Trends Ecol. Evol.*, *11*(9), 378–383, 1996.

Hansen, M. C., R. S. DeFries, J. R. G. Townshend, and R. Sohlberg, Global land cover classification at 1 km spatial resolution using a classification tree approach, *Int. J. Remote Sens.*, *21*(6–7), 1331–1364, 2000.

Hartigan, J. A., *Clustering Algorithms*, 351 pp., John Wiley, New York, 1975.

Hicke, J. A., G. P. Asner, J. T. Randerson, C. Tucker, S. Los, R. Birdsey, J. C. Jenkins, C. Field, and E. Holland, Satellite-derived increases in net primary productivity across North America, 1982–1998, *Geophys. Res. Lett.*, 10.1029/2001GL013578, in press, 2002.

Houghton, R. A., J. L. Hackler, and K. T. Lawrence, The U.S. carbon budget: Contributions from land-use change, *Science*, *285*, 574–578, 1999.

Huffman, G. J., R. F. Adler, P. Arkin, A. Chang, R. Ferraro, A. Gruber, J. Janowiak, A. McNab, B. Rudolf, and U. Schneider, The Global Precipitation Climatology Project (GPCP) combined precipitation data set, *Bull. Am. Meteorol. Soc.*, *78*(1), 5–20, 1997.

Keeling, C. D., J. F. S. Chin, and T. P. Whorf, Increased activity of northern vegetation inferred from atmospheric CO_2 measurements, *Nature*, *382*, 146–149, 1996.

Kistler, R., et al., The NCEP-NCAR 50-year reanalysis: Monthly means CD-ROM and documentation, *Bull. Am. Meteorol. Soc.*, *82*(2), 247–267, 2001.

Knapp, A. K., and M. D. Smith, Variation among biomes in temporal dynamics of aboveground primary production, *Science*, *291*, 481–484, 2001.

Lobell, D. B., J. A. Hicke, G. P. Asner, C. B. Field, C. J. Tucker, and S. O. Los, Satellite estimates of productivity and light use efficiency in United States agriculture, 1982–1998, *Global Change Biol.*, in press, 2002.

Los, S. O., G. J. Collatz, P. J. Sellers, C. M. Malmstrom, N. H. Pollack, R. S. DeFries, L. Bounoua, M. T. Parris, C. J. Tucker, and D. A. Dazlich, A global 9-yr biophysical land surface dataset from NOAA AVHRR data, *J. Hydrometeorol.*, *1*, 183–199, 2000.

Malmström, C. M., M. V. Thompson, G. P. Juday, S. O. Los, J. T. Randerson, and C. B. Field, Interannual variation in global-scale net primary production: Testing model estimates, *Global Biogeochem. Cycles*, *11*, 367–392, 1997.

Mickler, R. A., R. A. Birdsey, and J. Horn, *Responses of Northern U.S. Forests to Environmental Change*, 578 pp., Springer-Verlag, New York, 2000.

Monteith, J. L., Climate and the efficiency of crop production in Britain, *Philos. Trans. R. Soc. London, Ser. B*, *281*, 277–294, 1977.

Myneni, R. B., C. D. Keeling, C. J. Tucker, G. Asrar, and R. Nemani, Increased plant growth in the northern high latitudes from 1981 to 1991, *Nature*, *386*, 698–702, 1997.

Nadelhoffer, K. J., B. A. Emmett, P. Gunderson, O. J. Kjonaas, C. J. Koopmans, P. Schleppi, A. Tietema, and R. F. Wright, Nitrogen deposition makes a minor contribution to carbon sequestration in temperate forests, *Nature*, *398*, 145–148, 1999.

Oechel, W. C., S. Cowles, N. Grulke, S. J. Hastings, B. Lawrence, T. Prudhomme, G. Riechers, B. Strain, D. Tissue, and G. Vourlitis, Transient nature of CO_2 fertilization in Arctic tundra, *Nature*, *371*, 500–503, 1994.

Oren, R., et al., Soil fertility limits carbon sequestration by forest ecosystems in a CO_2-enriched atmosphere, *Nature*, *411*, 469–472, 2001.

Pacala, S. W., et al., Consistent land- and atmosphere-based U. S. carbon sink estimates, *Science*, *292*, 2316–2320, 2001.

Potter, C. S., J. T. Randerson, C. B. Field, P. A. Matson, P. M. Vitousek, H. A. Mooney, and S. A. Klooster, Terrestrial ecosystem production: A process model based on global satellite and surface data, *Global Biogeochem. Cycles*, *7*, 811–842, 1993.

Potter, C. S., S. Klooster, and V. Brooks, Interannual variability in terrestrial net primary production: Exploration of trends and controls on regional to global scales, *Ecosystems*, *2*, 36–48, 1999.

Randerson, J. T., C. B. Field, I. Y. Fung, and P. P. Tans, Increases in early season ecosystem uptake explain recent changes in the seasonal cycle of atmospheric CO_2 at high northern latitudes, *Geophys. Res. Lett.*, *26*(17), 2765–2768, 1999.

Ruimy, A., G. Dedieu, and B. Saugier, Methodology for the estimation of terrestrial net primary production from remotely sensed data, *J. Geophys. Res.*, *99*(D3), 5263–5284, 1994.

Ryan, M. G., D. Binkley, and J. H. Fownes, Age-related decline in forest productivity: Pattern and process, *Adv. Ecol. Res.*, *27*, 213–262, 1997.

Schimel, D., I. G. Enting, M. Heimann, T. M. L. Wigley, D. Raynaud, D. Alves, and U. Siegenthaler, CO_2 and the carbon cycle, in *Climate Change 1994: Radiative Forcing of Climate Change and an Evaluation of the IPCC IS92 Emission Scenarios*, edited by J. T. Houghton et al., pp. 33–71, Cambridge Univ. Press, New York, 1995.

Schimel, D., et al., Contribution of increasing CO_2 and climate to carbon storage by ecosystems in the United States, *Science*, *287*, 2004–2006, 2000.

Schlesinger, W. H., *Biogeochemistry: An Analysis of Global Change*, 588 pp., Academic, San Diego, Calif., 1997.

Sheffield, R. M., and J. G. Dickson, The south's forestland: On the hot seat to provide more, in *Transactions of the 63rd North American Wildlife and Natural Resources Conference*, pp. 316–331, Wildlife Manage. Inst., Orlando, Fla., 1998.

Smith, S. D., T. E. Huxman, S. F. Zitzer, T. N. Charlet, D. C. Housman, J. S. Coleman, L. K. Fenstermaker, J. R. Seemann, and R. S. Nowak, Elevated CO_2 increases productivity and invasive species success in an arid ecosystem, *Nature*, *408*, 79–82, 2000.

Smith, W. B., J. L. Vissage, R. Sheffield, and D. R. Darr, Forest resources of the United States, report, U.S. Dep. Agric. For. Serv., N. Cent. For. Exp. Stn., St. Paul, Minn., in press, 2002.

Thompson, M. V., J. T. Randerson, C. M. Malmström, and C. B. Field, Change in net primary production and heterotrophic respiration: How much is necessary to sustain the terrestrial carbon sink?, *Global Biogeochem. Cycles*, *10*, 711–726, 1996.

Townsend, A. R., B. H. Braswell, E. A. Holland, and J. E. Penner, Spatial and temporal patterns in terrestrial carbon storage due to deposition of fossil fuel nitrogen, *Ecol. Appl,*, *6*(3), 806–814, 1996.

Tucker, C. J., D. A. Slayback, J. E. Pinzon, S. O. Los, R. B. Myneni, and M. G. Taylor, Higher northern latitude NDVI and growing season trends from 1982 to 1999, *Int. J. Biometeorol.*, *45*, 184–190, 2001.

U.S. Department of Agriculture Forest Service, Forest Service Resource Inventories: An Overview, report, 39 pp., U.S. Dep. Agric. For. Serv., Washington, D. C., 1992.

VEMAP members, Vegetation/ecosystem modeling and analysis project: Comparing biogeography and biogeochemistry models in a continental-scale study of terrestrial ecosystem responses to climate change and CO_2 doubling, *Global Biogeochem. Cycles*, *9*, 407–438, 1995.

Williams, D. W., and A. M. Liebhold, Spatial scale and the detection of density dependence in spruce budworm outbreaks in eastern North America, *Oecologia*, *124*(4), 544–552, 2000.

G. P. Asner, C. Field, and J. A. Hicke, Carnegie Institution of Washington, 260 Panama Street, Stanford, CA 94305, USA. (greg@globalecology.stanford.edu; chris@globalecology.stanford.edu; jhicke@globalecology.stanford.edu)

R. Birdsey, U.S. Department of Agriculture Forest Service, 11 Campus Boulevard, Suite 200, Newtown Square, PA 19073, USA. (rbirdsey@fs.fed.us)

J. C. Jenkins, U.S. Department of Agriculture Forest Service, P. O. Box 968, Burlington, VT 05402, USA. (jjenkins@fs.fed.us)

S. Los, University of Wales, Singleton Park, Swansea, SA2 8PP, UK. (s.o.los@Swansea.ac.uk)

J. T. Randerson, Divisions of Geological and Planetary Sciences and Engineering and Applied Science, California Institute of Technology, 101 North Mudd, Mail Stop 100-23, Pasadena, CA 91125, USA. (jimr@gps.caltech.edu)

C. Tucker, NASA Goddard Space Flight Center, Laboratory for Atmospheric Physics, Code 923, Greenbelt, MD 20771, USA. (Compton@kratmos.gsfc.nasa.gov)

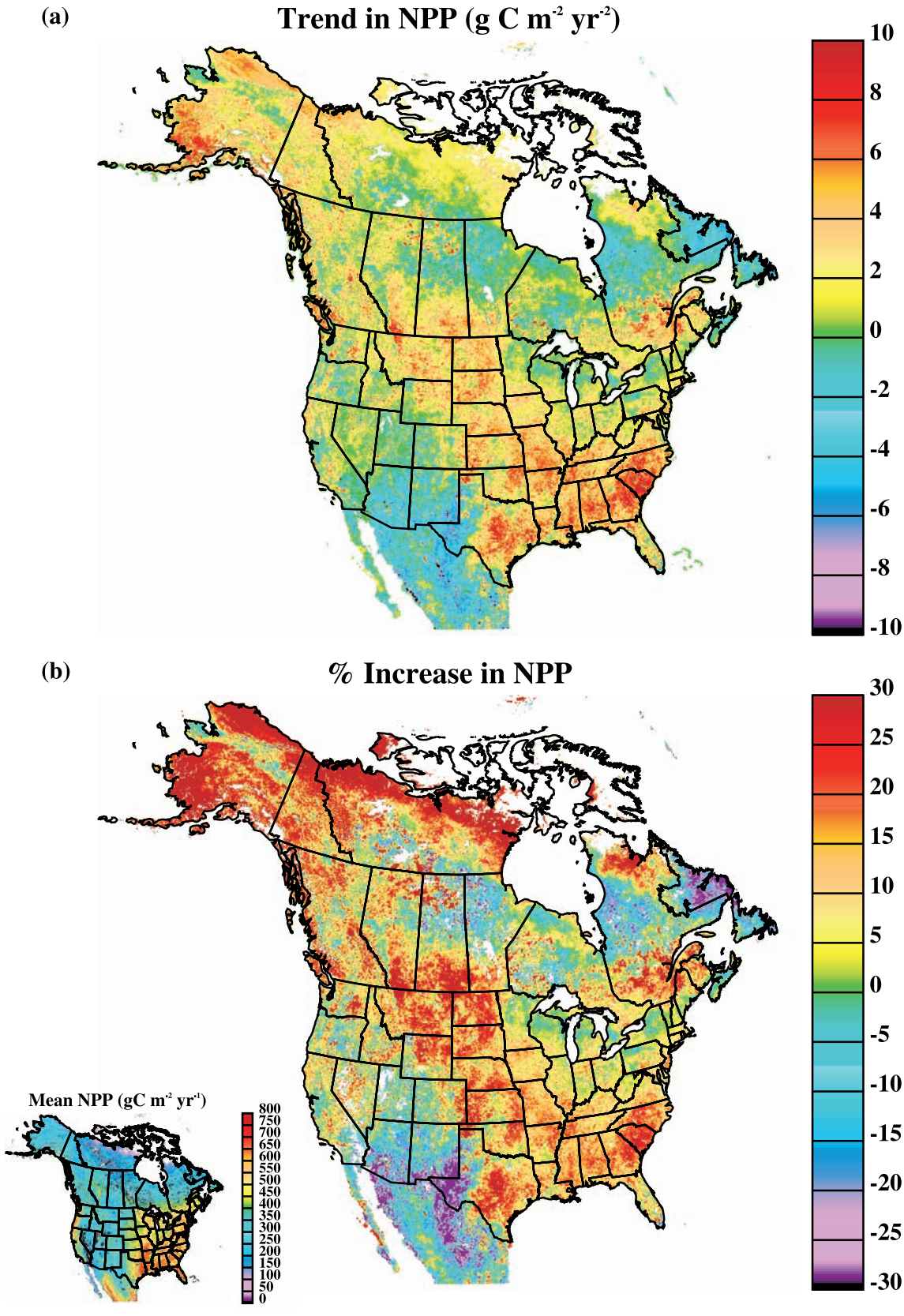

Figure 1. (a) Trends in net primary productivity (NPP, in g C m^{-2} yr^{-2}), 1982–1998. (b) Percentage increase in NPP, computed by multiplying the linear trend at each location by the number of years in the time period (17), then dividing by the 1982 NPP. Inset shows mean annual NPP (in g C m^{-2} yr^{-1}) (taken from Hicke et al., submitted manuscript, 2001).

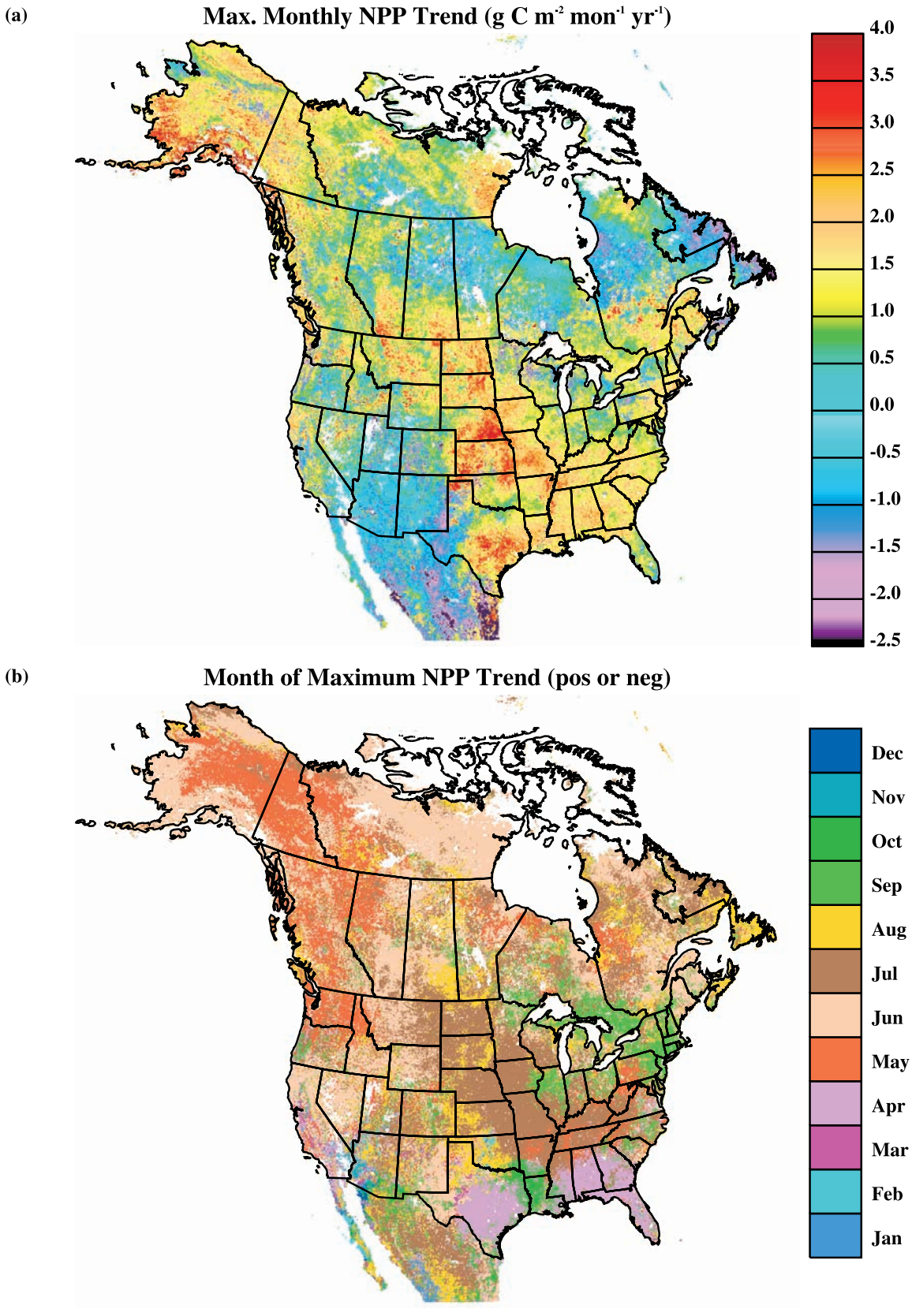

Figure 4. (a) Maximum monthly trend in net primary productivity (NPP, in g C m^{-2} $month^{-1}$ yr^{-1}). Monthly trends were computed for each month (January, February, etc.), generating an annual cycle of monthly trends at each point. This plot shows the maximum absolute value (positive or negative) of the monthly trends at each point. (b) Month when maximum absolute value (positive or negative) of monthly NPP trend occurred.

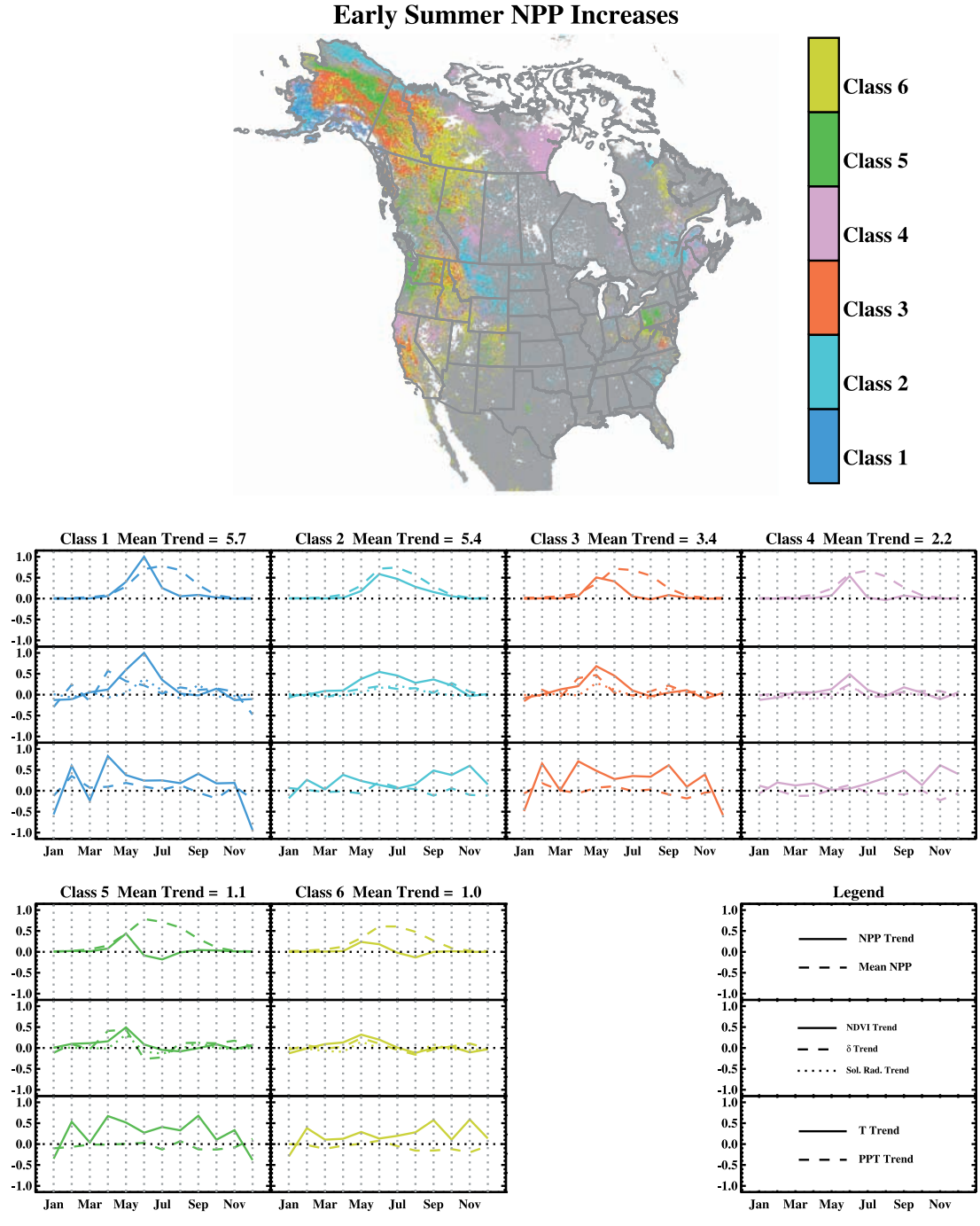

Figure 5. Results of a classification based on monthly net primary productivity (NPP) and climate trends; see text for details of the method. (Top) Map of locations of Classes 1–6, which have early summer NPP increases. (Bottom) Annual cycle of variables associated with each class, averaged across all points associated with that class. Top panel in each plot shows mean monthly trend in NPP (solid curve) and mean monthly NPP (dashed curve). Middle panel in each plot shows trends in NDVI (solid curve), climate down-regulator δ (dashed curve), and solar radiation (dotted curve). Bottom panel in each plot shows mean monthly trends in temperature (solid curve) and precipitation (dotted curve). All variables are normalized by largest value across classes.

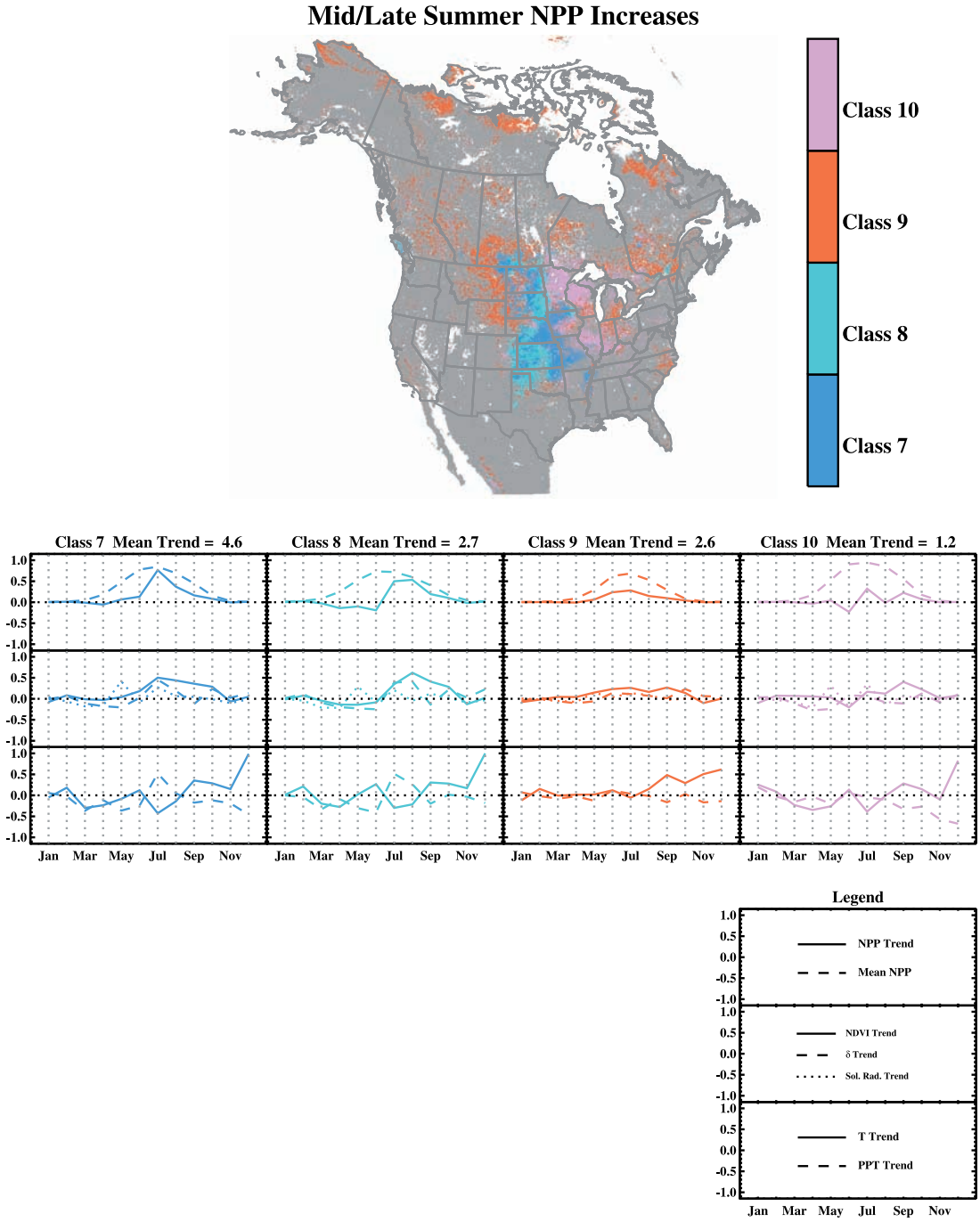

Figure 6. Same as Figure 5, but for classes with mid- and/or late summer increases in NPP.

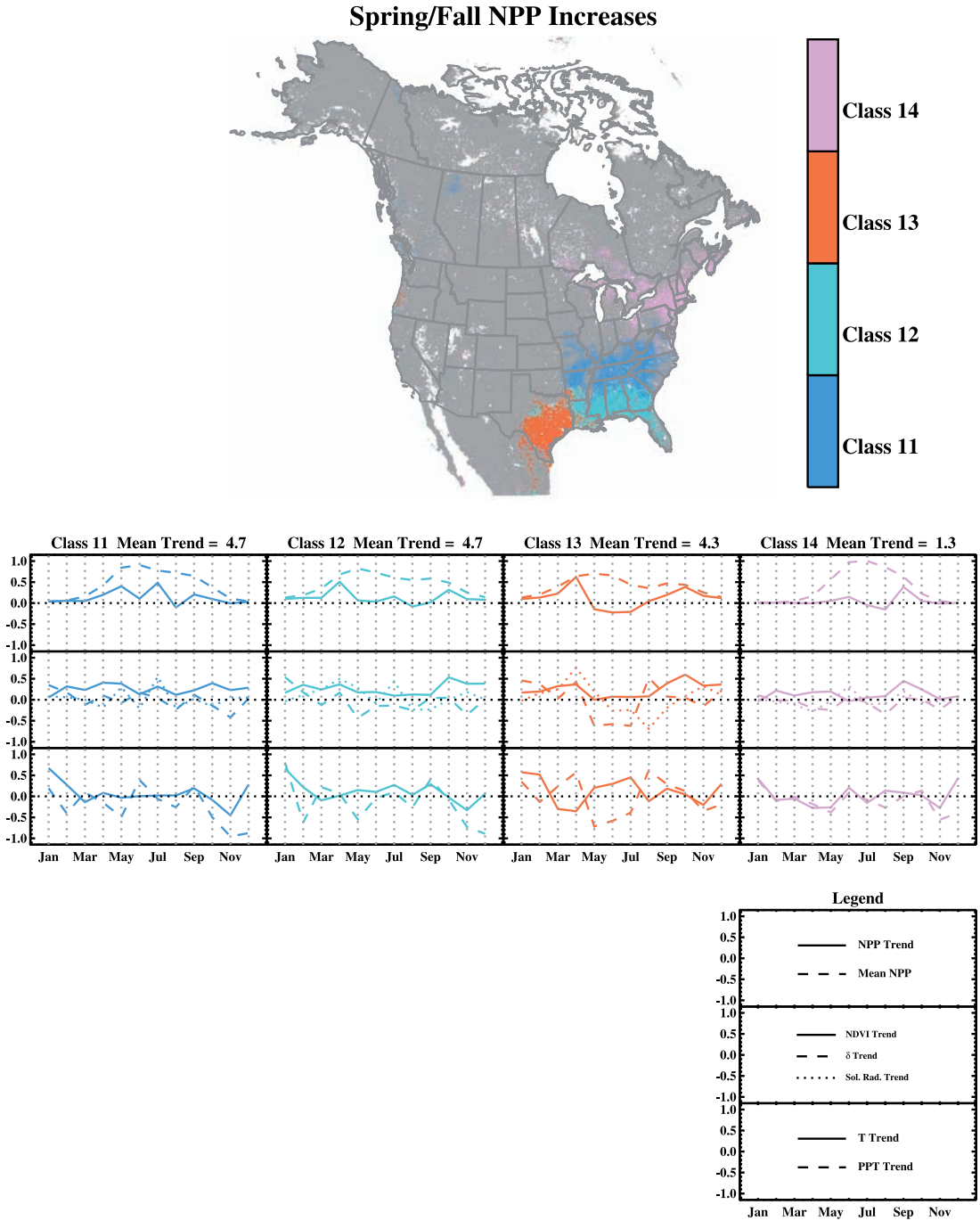

Figure 7. Same as Figure 5, but for classes with spring and fall increases in NPP.

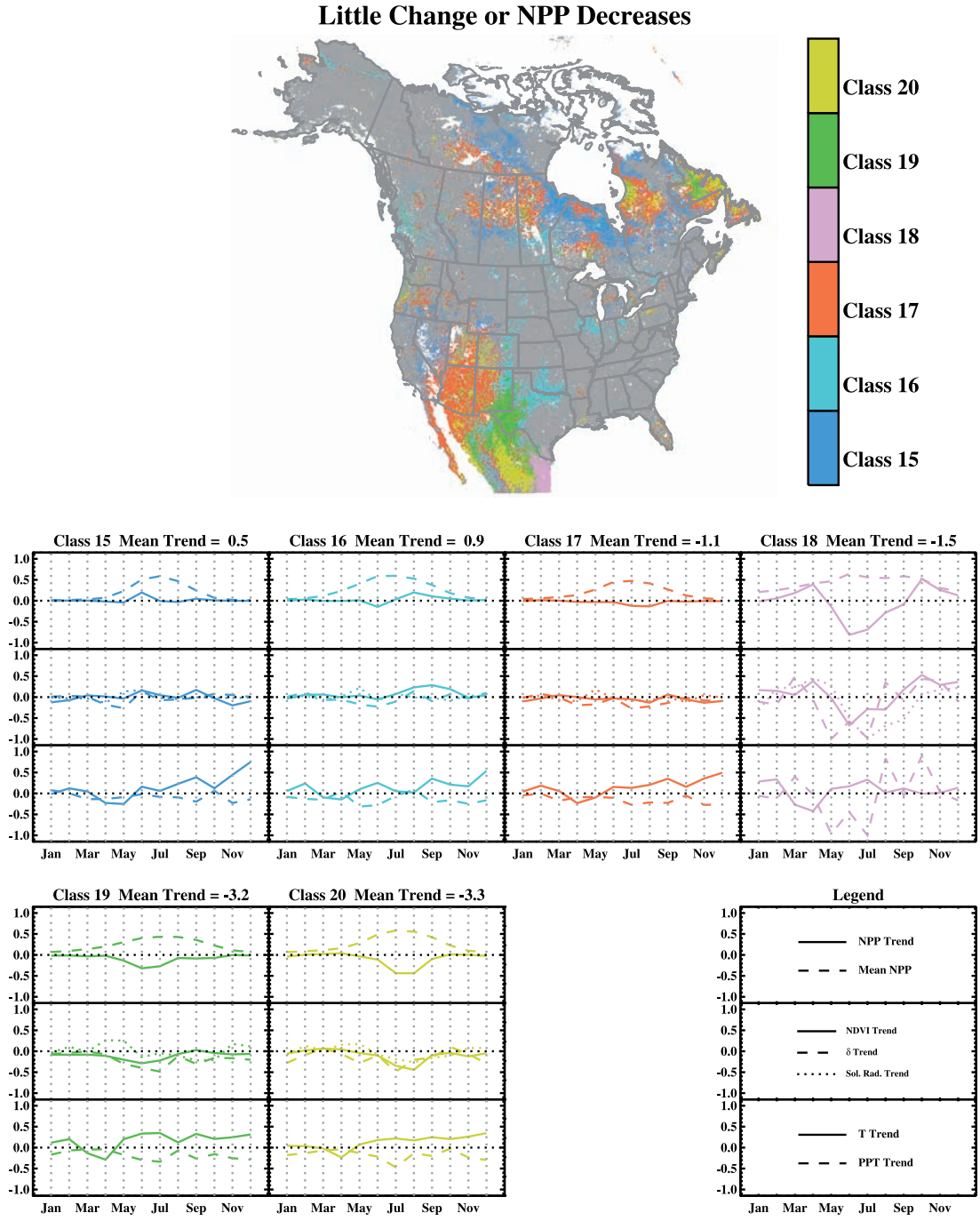

Figure 8. Same as Figure 5, but for classes with little change or decreases in NPP.

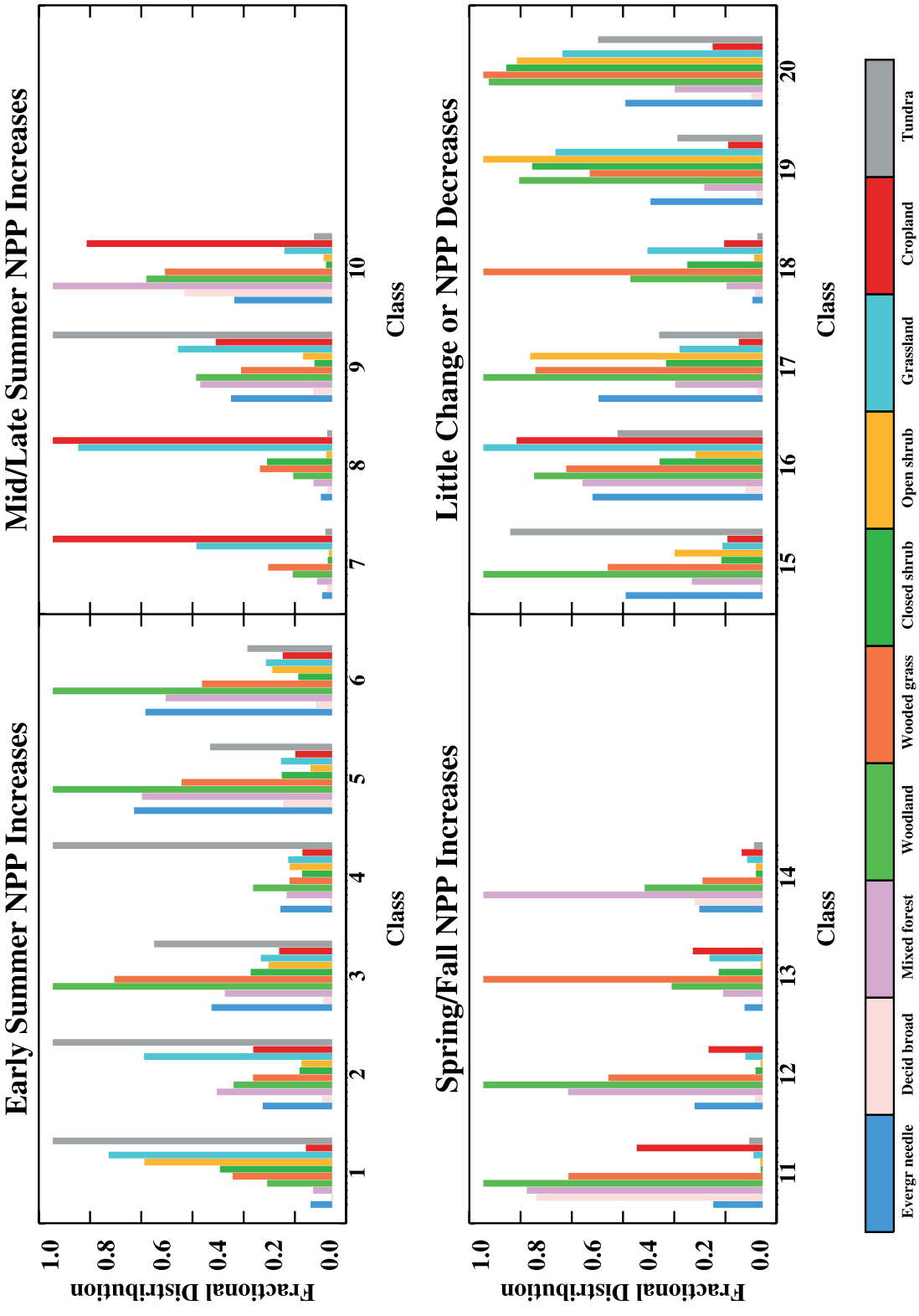

Figure 9. Fractional frequency distribution of biomes within each class.

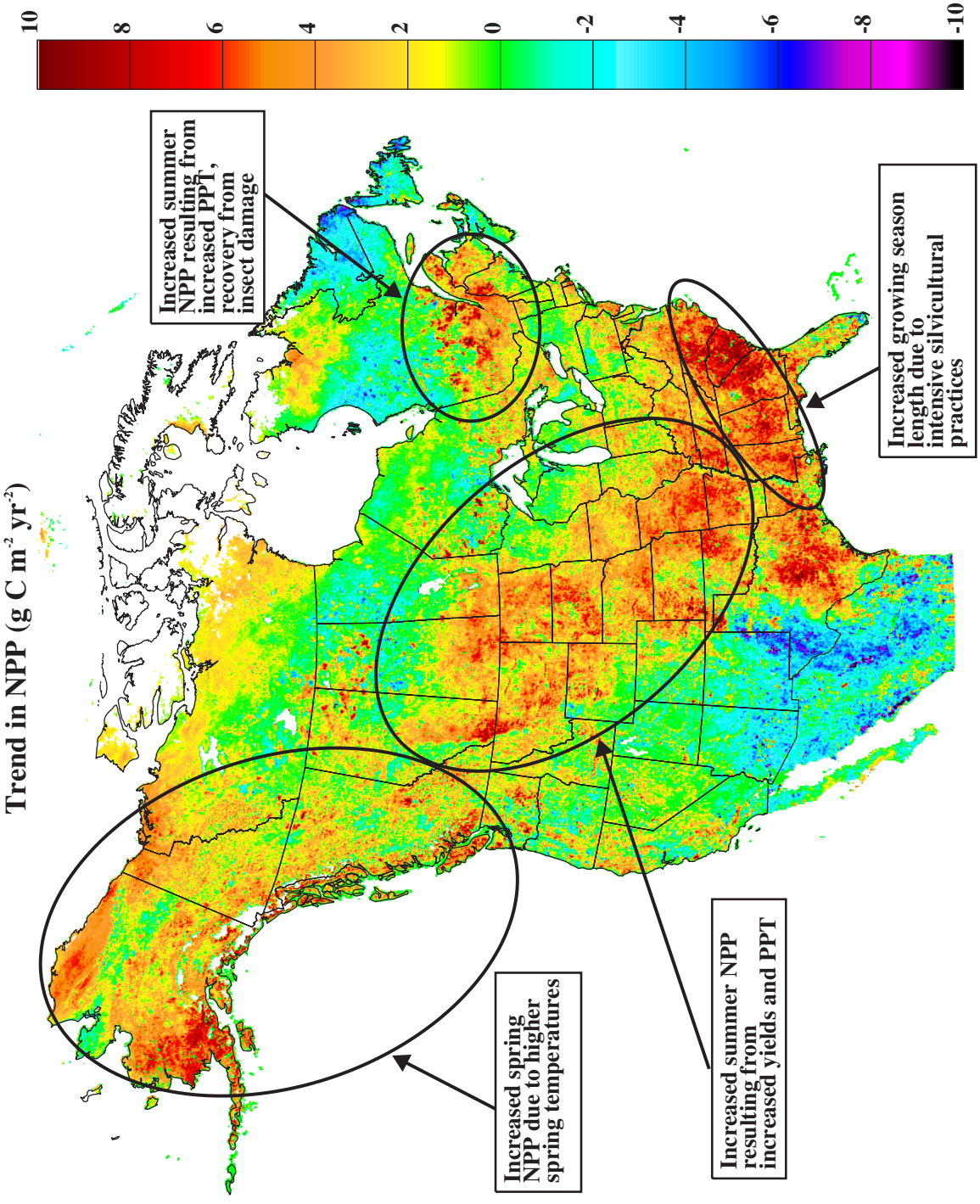

Figure 10. Same as Figure 1a, with additional summaries of regions where NPP has increased. Seasonal timing of NPP increase is indicated as well as possible explanations (CO_2 fertilization is not considered).